



21 then analyzed to produce the geodiversity of Crete. The geodiversity map is used to quantify the  
22 geodiversity, by calculating landscape diversity and other spatial pattern indices. Those indices  
23 are evaluating the richness, evenness, fragmentation and shape of the landscape patch types. The  
24 outcome of this study has highlighted that western Crete is characterized by complex  
25 geodiversity with more irregular, elongated and fragmented landscape patterns relative to the  
26 eastern part of the island. The geodiversity indices provide insights into the processes shaping  
27 landscapes, particularly the "battle" between neotectonic landscape deformation and  
28 erosion/deposition. The methodology presented can be useful for decision makers when  
29 evaluating a regions geological heritage, planning the management of natural resources, or  
30 designating areas for conservation.

31

32 **Keywords:** Geodiversity; geomorphometrics; landscape indices; geoinformatics; ASTER G-  
33 DEM.

34

35

## 1. Introduction

36 Various physical properties of the Earth's surface are factors that influence local  
37 topography, with geomorphometric landform information providing valuable knowledge  
38 regarding the interfered processes shaping landscapes and producing geodiversity (Nieto, 2001;  
39 Benito-Calvo et al., 2009). Gray (2004) defined geodiversity as: "*The natural range (diversity) of*  
40 *geological (rocks, minerals, fossils), geomorphological (landform processes) and soil features. It*  
41 *includes their assemblages, relationships, properties, interpretations and systems.*" Kozlowksi  
42 (2004), added surface waters such as lakes and rivers, as well as including the impact of human

43 influence on geodiversity. Sharples (2002) also considered the interrelated character of the  
44 assemblages, properties, systems and processes of the geological, geomorphological and soil  
45 elements that produce geodiversity. The geodiversity concept has been used in various  
46 applications such as geological heritage, geoconservation, ecosystem management, etc (e.g.  
47 Gray, 2004, Carcavilla et al., 2008; Gordon et al., 2012; Stavi et al., 2015). The subject of  
48 geodiversity has not been as widely well-established or used as a biodiversity concept. So it  
49 follows that the abiotic diversity of Earth remains a relatively challenging domain to assess both  
50 qualitatively and quantitatively (Pereira et al., 2013).

51         Although the concept of geodiversity has been widely discussed, there are relatively few  
52 publications on the quantification of geodiversity (e.g. Bruschi, 2007; Serrano and Ruiz-Flano,  
53 2007; Benito-Calvo et al., 2009; Ruban 2010). Pioneering work involving the classification of  
54 geodiversity was carried out in the development of land systems mapping (Christian and Stewart,  
55 1952; Ollier et al., 1969) and by researchers analyzing landscape parametrics (e.g. Leopold,  
56 1969; Conacher and Dalrymple, 1977). However there has been a resurgence of geodiversity  
57 research in recent years due to improved computing and software functionality, which via the  
58 geoinformatics has provided a useful tool for managing natural resources, human resources and  
59 natural hazards (e.g. Serrano and Ruiz-Flano, 2007; Parks and Mulligan, 2010; Hjort and Luoto,  
60 2012; Rawat, 2013). Investigating heterogeneity in geological and geomorphological properties  
61 can lead to the quantification of landscapes and towards a better understanding of their  
62 complexity (Nieto, 2001; Panizza and Piacente, 2008). Physical elements such as  
63 geomorphological and geological attributes, constitute the main geodiversity elements in its  
64 assessment (Kozlowski, 2004; Serrano and Ruiz-Flano, 2007). A combination of geological,  
65 geomorphological, climatic or hydrological information using geoinformatic approaches can be

66 useful in the quantification of geodiversity for a regional scale (Benito-Calvo et al., 2009; Hjort  
67 and Luoto, 2010).

68 This study aims to assess the geodiversity of Crete, one of the most tectonically active  
69 areas in the world (Pirazzoli et al., 1996). The region is characterized by a high degree of  
70 neotectonic activity which is the main triggering agent for the development of a complex  
71 heterogeneous terrain (Shaw et al., 2008). In order to assess and describe the abiotic  
72 heterogeneity, this study quantifies the geodiversity of Crete, based on a regional geodiversity  
73 map that includes geomorphometric, geological, hydrological and climatic information. Such  
74 information can constitute the main factors in evaluating the geodiversity of a region, adopting  
75 the methodology of Benito-Calvo et al. (2009), which is partly modified to fit the needs of this  
76 study.

77 The small number of variables used by Benito-Calvo et al. (2009) to study the  
78 tectonically more “quiet” region of Spain in comparison to Crete, leaves scope for more  
79 geomorphometric indices to be used for a deeper investigation of the geomorphological,  
80 hydrological and morphotectonic context of Crete. The final geomorphometric classification of  
81 this study considers additional hydrological and morphotectonic indices that Benito-Calvo et al.  
82 (2009) did not use in their study. The geomorphometric classification was based on  
83 geomorphometric indices (amplitude of relief (*Ar*), stream length gradient (*SL*), stream frequency  
84 (*Fu*), drainage density (*Dd*), elevation relief (*Er*), topographic wetness index (*TWI*), slope  
85 gradient (*Sg*), surface area/ratio (*SAR*), dissection index (*Di*)); all derived from the ASTER G-  
86 DEM, a freely-available digital elevation model with 30m pixels. The geomorphometric indices  
87 were spatially analyzed to provide a map of geomorphometric classes. The geological  
88 classification was based on digitized 1:50,000 scale geological maps (IGME, 1971), with the

89 geological classification simplifying litho-chronologically, the initial complex formations of the  
90 IGME (1971) geological maps. The climatic classification consisted of seasonal average  
91 temperature and rainfall raster data layers for the period 1930-2000, determined by the EMERIC  
92 project (Sarris, 2007; Fassoulas et al., 2007). Two different widely used approaches were tested  
93 in this study, the one by Chorley et al. (1984) for evaluating morphogenetic regions and the one  
94 of Kottek et al. (2006) providing an update of Köppen-Geiger studies for climatic zones  
95 determination (Köppen, 1936; Geiger, 1954). The results of the Chorley et al. (1984) approach  
96 did not show significant variation of morphogenetic regions, with almost the whole island being  
97 characterized as “arid” so the Kottek et al. (2006) methodology was preferred, offering a larger  
98 variance of climatic zones across Crete. Each of the aforementioned classifications, presented in  
99 detail below, were implemented using GIS softwares to obtain a regional geodiversity map of  
100 Crete, via an overlay union procedure (Benito-Calvo et al., 2009). In that way, all geodiversity  
101 components were assessed equally, avoiding overestimation of any particular components  
102 (Pereira et al., 2013).

103 Landscape metrics were then applied on the geodiversity map to quantify the  
104 geodiversity, following Benito-Calvo et al. (2009). This study used calculations of diversity  
105 indices which can determine the heterogeneity of landscapes, via indices such as the Patch  
106 Richness Density (PRD), Shannon’s Diversity Index (SHDI), Shannon’s Evenness Index (SHEI),  
107 Simpson’s Diversity Index (SIDI) and Simpson’s Evenness Index (SIEI). In the study of Benito-  
108 Calvo (2009), they acknowledge that the combination of the aforementioned diversity indices  
109 with other spatial pattern indices will lead to better comprehension of the landscape spatial  
110 configuration. For this reason additional spatial pattern indices, such as: i) shape index (*SHAPE*);  
111 ii) proximity index (*PROX*); iii) related circumscribing circle (*CIRCLE*); iv) patch density (*PD*)

112 and; v) perimeter-area fractal dimension (*PAFRAC*), were also calculated to evaluate the  
113 landscape form regarding the shape and fragmentation characteristics. Those indices were  
114 analyzed using Fragstats spatial pattern analysis freeware (McGarigal et al., 2002). The  
115 quantification, classification and mapping of geological, geomorphological, hydrological and  
116 climatic factors, can improve our understanding of the processes and materials that have  
117 controlled landscape evolution across Crete. Such knowledge is new for the region offering  
118 valuable information to various scientific fields for decision making, such as land use mapping,  
119 geological heritage, environmental management or nature conservation.

120

121

## 2. Study area

122 Crete lies within the emergent outer fore-arc of the largest and most active subduction  
123 zone in Europe, the Hellenic arc and is therefore characterized by high rates of tectonic activity  
124 and seismicity (Papazachos and Comninakis, 1978; Kellat, 1996; Pirazzoli, 2005) (Fig. 1). By  
125 way of an example, the 21 July AD 365 earthquake (Mw 8.3-8.5), the “Early Byzantine  
126 Tectonic Paroxysm”, produced co-seismic uplift up to 9 meters on southwestern Crete  
127 (Pirazzoli et al., 1996; Stiros, 2001; Shaw et.al, 2008). The island is characterized by low to  
128 medium elevation (up to ~900m) on its northern coast and high elevation (up to ~2500m) with  
129 steep slopes on the southern coast, with N-S trending deeply incised valleys (Fytrolakis, 1980;  
130 Sarris, 2005). Two large massifs, the Lefka Ori and Psiloritis mountains, are found in the western  
131 and central part of the island, with peaks of up to ~2500 m (Fig. 1: labeled as LO and P  
132 respectively). The geological and tectonic setting of the island was initially investigated in  
133 the early 1950s (Papastamatiou & Reichel, 1956; Papastamatiou et al., 1959). These studies  
134 indicated the presence of two major nappes, the Pindos nappe overlying the Tripolis nappe

135 unit. These units belong to the external Hellenides and were deformed after the deposition of  
136 flysch formations in the Late Eocene-Oligocene (Renz, 1955; Aubouin and Dercourt, 1970).  
137 Further work in the 1970s established a better tectonostratigraphic framework for Crete by  
138 indicating the presence of several nappes, either below the Tripolis unit or above the Pindos  
139 nappe (Seidel, 1971; Baumann et al., 1976). The geological setting of the island of Crete is very  
140 complex and it is characterized by pre-Alpine and Alpine rocks (composing a pile of nappes) and  
141 post-Alpine rocks (Neogene and Quaternary sediments) (Fig. 2). In the case of pre-Alpine and  
142 Alpine rocks, the Cretan nappe pile consists of two nappe groups: i) the upper nappes (Tripolis,  
143 Pindos, Uppermost) and; ii) the lower nappes (Plattenkalk, Trypali, Phyllite/Quartzite). In the  
144 post-Alpine rocks, the sediments of Crete can be divided into six groups: i) Prina group, ii) Tefeli  
145 group, iii) Vrysses group, iv) Hellenikon group, v) Finikia group, and vi) Agia Galini group  
146 (Meulenkamp et al., 1979).

147

148

### 3. Methods and Datasets

#### 149 3.1 Regional Geodiversity

##### 150 i) *Geomorphometric classification*

151 In order to determine geomorphometric classification, several geomorphometric variables  
152 extracted from the ASTER G-DEM were evaluated (Fig. 3). In a similar study, Benito-Calvo et  
153 al. (2009) examined only the variables of elevation, slope, tangential curvature and roughness to  
154 perform a geomorphometric classification. In order to highlight additional geomorphological,  
155 hydrological and morphotectonic information for this tectonically active region, various other  
156 variables were analyzed in this study. The geomorphological information was mainly derived by

157 indices, such as *SAR*, *Sg*, *Er* and *Di*, highlighting the terrain roughness, dissection, concavity or  
158 convexity (Singh and Dubey, 1994; Jenness, 2004; Rowberry, 2012) (Fig. 4). The  
159 morphotectonic information was contributed prior by indices such as *Ar*, *SL* (Ciccacci et al.,  
160 1988; Toudeshki and Arian, 2011) (Fig. 4). Some supplementary indices such as *Dd*, *Fu* and *TWI*  
161 were acknowledged to provide hydrological information while their interrelation can also  
162 highlight both geomorphological and morphotectonic information (Kouli et al., 2007; Argyriou  
163 et al., 2016) (Fig. 4). The indices to be used in the geomorphometric classification were derived  
164 after prior evaluation of the low interdependency of various DEM derivatives by selecting the  
165 non-correlated ones (Table 1). The following geomorphometric indices and their contributed  
166 geomorphological, hydrological and morphotectonic information were considered:

167       The *amplitude of relief (Ar)* is the maximum difference in elevation within unit areas, in  
168 this case, 1 km<sup>2</sup> (Ciotoli et al., 2003) (Fig. 4). *Ar* is useful for assessing active tectonics to  
169 determine recent vertical displacements (Ciccacci et al., 1988; Troiani and Della Seta, 2008) and  
170 can also be used to determine fluvial erosion (Della Seta et al, 2004). Following the method of  
171 Della Seta et al. (2004), the relative relief was determined by subtraction of the ASTER G-  
172 DEM<sub>max</sub> (each output cell contains the maximum of the input cells that are encompassed by the  
173 extent of that cell) from the ASTER G-DEM<sub>min</sub> (each output cell contains the minimum of the  
174 input cells that are encompassed by the extent of that cell), within a grid of 1×1 km cells  
175 (Argyriou et al., 2016). The *Ar* values were determined by the centroid points of each unit area,  
176 while kriging was used as the interpolation method, to produce a spatial distribution map of *Ar*  
177 (Troiani and Della Seta, 2008). The higher values of the *Ar* index imply to vertical displacements  
178 of uplifted or subsidence blocks, while regions with no intense landscape deformation are  
179 highlighted by their low values (Ciccacci et al., 1988; Argyriou et al., 2016).



180           The *stream length gradient (SL)* shows the change in elevation of a reach, relative to the  
181 length of that reach, multiplied by the total length of the channel from the point where the index  
182 is being calculated (Hack, 1973; Keller, 1986; Toudeshki and Arian, 2011) (Fig. 4). Tectonic  
183 activity and rock resistance to erosion are the main factors that can be investigated using the *SL*  
184 index (Keller and Pinter, 1996; Garcia-Tortosa et.al, 2008). Any abrupt changes in the gradient  
185 of river will be revealed by the high values of the *SL* index and can be linked to active tectonics,  
186 while lower index values imply a fine drainage network without any influence of landscape  
187 deformation (Garcia-Tortosa et.al, 2008). The stream network was delineated from the ASTER  
188 G-DEM, by filling the voids using the D8 algorithm and the ArcGIS hydrology module to extract  
189 drainage network. A flow accumulation threshold value of  $400\text{m}^2$  provided the best fit for  
190 drainage network delineation, based on examination of satellite images, aerial photographs and  
191 topographical maps to determine vegetation corridors along floodplains (Tarboton et al., 1988;  
192 Maidment, 2002; Li, 2014; Argyriou et al., 2016).

193           *Stream frequency (Fu)* evaluates the total number of the stream segments to the area of  
194 the basin (Horton, 1945) (Fig. 4). The values of *Fu* indicate the degree of slope steepness, rock  
195 permeability and surface runoff. High *Fu* values ( $>5$ ) are associated with impermeable surface  
196 material, high relief and low infiltration capacity, while low *Fu* values imply permeable surface  
197 material, low relief and high infiltration capacity (Reddy et al., 2004; Ozdemir and Bird, 2009;  
198 Bagyaraj and Gurugnanam, 2011). The high *Fu* values can be indicative for areas with coarse  
199 drainage network and with the distortion of the drainage system being a result of neotectonic  
200 forces (Kouli et al., 2007). This index was calculated within a GIS software package by using  
201 kernel density within a search area of 2 km for the derived drainage network (Zavoianu, 1985;  
202 Kouli et al., 2007).

203            *Drainage density (Dd)* determines the total stream length, relative to the area of the basin  
204 (Horton, 1945) (Fig. 4). *Dd* provides information about surface runoff potential, the degree of  
205 landscape dissection, rock permeability and resistance to erosion can be assessed (Verstappen,  
206 1983; Tucker and Bras, 1998; Mesa, 2006). *Dd* is controlled by factors such as slope gradient  
207 and relative relief: low values (ie, < 5) are associated with a coarse drainage network, low relief,  
208 permeable surface material and terrain with long hill slopes (Berger and Entekhabi, 2001;  
209 Sreedevi, 2009). High *Dd* values indicate fine drainage texture, high relief, impermeable surface  
210 material and a dissected terrain (Strahler, 1964; Awasthi et al., 2002).

211            *Elevation relief (Er)* describes rugosity in a continuous raster surface and provides  
212 hypsometric information about a watershed (Pike and Wilson, 1971) (Fig. 4). It is equivalent to  
213 the hypsometric integral and can indicate the degree of disequilibrium in the balance of erosive  
214 and tectonic forces (Strahler, 1952, 1958; Luo, 1998; Keller and Pinter, 2002). The *Er* indicates  
215 the degree of landscape dissection (Clarke, 1966; Evans, 1972). Using *Er*, it is possible to  
216 discriminate lowland plains and dissected upland plateaus in a manner that cannot be achieved  
217 using slope angle or relative relief. A value near to 0 is indicative of concavity or sub-horizontal  
218 terrain with some isolated peaks, whereas a value near to 1 is indicative of convexity or sub-  
219 horizontal terrain with deep incision (Rowberry, 2012).

220            The *Topographic Wetness Index (TWI)* evaluates the soil moisture and surface saturation  
221 that is influenced by the changes in slope position such as shedding slopes or receiving slopes  
222 (Beven and Kirkby, 1979; Sorensen, 2005) (Fig. 4). The accumulation of water at the foot of  
223 slopes leads to a straight dependent relation with this index. It can also identify regions with low  
224 values indicating: i) V-shaped valleys characterized by high incision; ii) high relief surfaces  
225 where moisture accumulation exists in lower degree and; iii) longitudinal ridges. The higher

226 values of the index can assess regions consisting of: i) low gradient surface and moisture  
227 accumulation at higher degree, or ii) alluvial deposits (Migon et al., 2013). The *TWI* can be  
228 useful in evaluating land surface water distribution due to topographic changes and landscape  
229 deformation (Anderson and Kneale, 1982; Hjerdt et al., 2004; Argyriou et al., 2016).

230 *Slope gradient (Sg)* shows the change occurring in elevation between each cell and its  
231 neighbors (ESRI, 2003) (Fig. 4). Flat surfaces are characterized by low values while a steep  
232 relief is indicated by the higher values.

233 The *surface area/ratio (SAR)* generates a surface area and surface ratio raster layer from  
234 the ASTER G-DEM data (Fig. 4). The cell values for the new raster reflect the surface area and  
235 the surface ratio (surface area / planimetric area) for the land area contained within that cell's  
236 boundaries (Jenness, 2004). They provide useful indices of topographic roughness and  
237 convolutedness, giving a more realistic estimate of the land area available in relation to the  
238 simple planimetric area (Berry, 2002; Jenness, 2004). Surface area grids may easily be  
239 standardized into *SAR* grids by dividing the surface area value for each cell by the planimetric  
240 area within that cell. High values of *SAR* will indicate a rough and dissected terrain while lower  
241 index values will highlight smoother ones of low roughness (McAdoo et al., 2004).

242 The *Dissection index (Di)* is the ratio between absolute relief and relative relief,  
243 indicating the degree of dissection or vertical erosion (Singh and Dubey, 1994) (Fig. 4). It is a  
244 useful index for the study of terrain dynamics and landscape evolution, particularly the  
245 interaction between erosion and deposition (Mukhopadhyay, 1984; Sen, 1993). Low values of *Di*  
246 indicate lack of vertical dissection/erosion and hence dominance of flat surface, while high *Di*  
247 values suggest highly dissected terrain with vertical escarpment of hill slope (Pareta et al., 2011).

248 Many researchers have shown that the aforementioned indices are effective indicators of  
249 the Earth's surface processes driving landscape evolution (e.g. Currado and Fredi, 2000;  
250 Jamieson et al., 2004; Toudeshki and Arian, 2011). A correlation coefficient matrix has been  
251 produced to validate the low interdependency of the nine selected variables (Table 1). The  
252 correlation coefficient matrix showed that the indices were characterized by low correlation to  
253 each other (values  $<0.6$ ). Consequently, selected indices can provide a range of variant  
254 information regarding the geomorphological, hydrological and morphotectonic context to the  
255 final geomorphometric classification.

256 The next step of the analysis was to carry out a geomorphometric classification of the  
257 nine variables using the Interactive Self-Organizing Data Analysis Technique (ISODATA)  
258 algorithm. In this stage, clustering of the multivariate data takes place using an initial clustering  
259 with a large number of classes, in order to determine the characteristics of the natural grouping  
260 of cells (Benito-Calvo et al., 2009). A clustering histogram analysis, with an initial cluster of 90  
261 classes, was selected for the nine variables (Fig. 5B). The number of classes was ten times larger  
262 than the nine variables being used herein, following Benito-Calvo et al. (2009), where 40 classes  
263 were considered for the four selected variables. The clustering histogram curve approach  
264 highlighted eight major geomorphometric classes, separated by natural breaks, as prior terrain  
265 units (Fig. 5B). The eight classes of the geomorphometric classification, provided a more  
266 detailed overview of the geomorphological, hydrological and morphotectonic properties, relative  
267 to the study of Benito-Calvo et al. (2009), where only geomorphological characteristics were  
268 acknowledged (Table 2, Fig. 5 A and C).

269 ii) *Climatic classification*

270 The climatic zones of Crete were derived from analysis of seasonal mean temperature  
271 (1950-2000) and rainfall (1930-2000), as raster data layers (Soupios et al., 2005; Sarris et al.,  
272 2006). The climatic classification was based on the update Koppen-Geiger approach suggested  
273 by Kottek et al., (2006), using monthly temperature averages and monthly precipitation totals, as  
274 raster data layers (Köppen, 1936; Geiger, 1954) (Fig. 3). Kottek et al. (2006) identified five main  
275 global climatic types: group *A*, tropical/megathermal; group *B*, dry (arid and semiarid); group *C*,  
276 temperate/mesothermal; group *D*, continental/microthermal and; group *E*, polar and alpine,  
277 (Table 3). According to specific precipitation/temperature criteria, each group consists of various  
278 subcategories. Group *C* is the one that characterizes Crete, with subgroups varying across the  
279 island (Fig. 6).

### 280 *iii) Geological classification*

281 The geological map from IGME (1971), consisting of 74 rock formations from different  
282 geological zones, was used in the *geological classification* (Fig. 3). These formations were  
283 simplified to 12 main geological units, based on their rock types (sedimentary, metamorphic,  
284 volcanic) and their age (Cenozoic, Mesozoic and Paleozoic), as determined by the EMERIC  
285 project (Sarris, 2007; Fassoulas et al., 2007) (Fig. 7 and Table 4). The dominant formations in  
286 Crete are sedimentary and metamorphic rocks of Cenozoic and Mesozoic age, with only the  
287 Plattenkalk nappe being of Paleozoic age (Table 4). For each of the twelve geological units, the  
288 areal extent of the overlying geomorphometric classes was calculated (Table 4).

### 289 *iv) Geodiversity classification*

290 The spatial datasets were combined using an overlay union procedure, producing a  
291 regional geodiversity map of 229 discrete classes (Benito-Calvo et al., 2009) (Fig. 8A).

292 Comparison of the occurrences, for the three spatial datasets used in the geodiversity map,  
293 highlights the distribution of the dominant geomorphometric, geological and climatic classes  
294 across Crete (Fig. 8B).

295 v) *Quantification of the geodiversity*

296 The geometric and spatial composition of landscapes can be evaluated to quantify the  
297 geodiversity of Crete. One of the operations is diversity, a landscape property, consisting of  
298 richness and evenness (Spellerberg and Fedor, 2003). The number of classes can be defined by  
299 the compositional component of diversity, *richness*; while the distribution of the area of different  
300 classes can be quantified via the *evenness* of the diversity. Specific parameters were calculated in  
301 order to assess the geodiversity (Fig. 3 and Table 5). The quantification of landscape  
302 heterogeneity across Crete was achieved by evaluating various diversity and spatial pattern  
303 indices, using the Fragstats pattern analysis freeware (McGarigal et al., 2002). The examined  
304 indices were: Patch Richness Density (*PRD*), Shannon's Diversity Index (*SHDI*), Simpson's  
305 Diversity Index (*SIDI*), Simpson's Evenness Index (*SIEI*) and Shannon's Evenness Index (*SHEI*)  
306 (Table 5). Some indices (e.g. *SHDI*) are more sensitive to richness than evenness (Shannon and  
307 Weaver, 1949). As a result, rare patch classes disproportionately influence the weighting of the  
308 index. For instance, *SIDI* is less sensitive to richness and as a result it disproportionately  
309 influences the weight of the common patch classes (Simpson, 1949). Large areas can have an  
310 increased richness, due to greater heterogeneity in comparison to smaller areas.

311 Evenness is the observed level of diversity, divided by the maximum possible diversity  
312 for a given patch richness: it is used to determine the distribution of area among patch classes. As  
313 evenness approaches 1, the observed diversity reaches perfect evenness; conversely, larger

314 values imply greater landscape diversity. The set of quantitative indices were evaluated for each  
315 district of Crete, regarding the geodiversity map and each factor individually (Table 6).

316 These diversity indices when combined with other spatial pattern indices can improve the  
317 understanding of the landscape spatial composition (Benito-Calvo et al., 2009). As Crete is  
318 characterized by a complex neotectonic status and a high degree of heterogeneity, extra spatial  
319 pattern indices were considered in this study to examine the complex landscape spatial  
320 composition and to quantify its shape and fragmentation characteristics. Those extra indices  
321 were: i) shape index (*SHAPE*); ii) proximity index (*PROX*); iii) related circumscribing circle  
322 (*CIRCLE*); iv) patch density (*PD*) and; v) perimeter-area fractal dimension (*PAFRAC*) (Table 5  
323 and 6). Such characteristics can be associated with the degree of neotectonic activity influencing  
324 an area, by highlighting any irregular, elongated and highly fragmented landscapes.

325

326

#### 4. Results

327 The geomorphometric classification was based on the nine thematic maps presented in  
328 Fig. 4. These maps were combined to derive eight geomorphometric classes (Fig. 5 and Table 2).  
329 The following observations were made for the geomorphometric classification, relative to the  
330 geological formations (Table 4 and Fig. 8B):

- 331 • More than half of the Quaternary (*Q.al*) coverage (~11% total area coverage) is found  
332 over coastal lands and plains (mean height: 108 m) with gentle slopes (mean:  $7.8^0$ ), low  
333 roughness, minimal dissection and minimal landscape deformation.

- 334 • The Neogene (*Mk*) formation (~29% total area coverage) is found mainly over plains and  
335 valleys with low relief, up to a mean height 371 m asl, with low roughness, minimal  
336 dissection and minimal landscape deformation.
- 337 • The Tripolis Flysch zone (*ft*) is characterized by geomorphometric classes 2, 3 and 4,  
338 occurring at mean heights of 371m asl, with variable dissection and roughness.
- 339 • The Pindos Flysch zone (*fo*) is characterized by similar geomorphometric classes to the  
340 Tripolis Flysch zone (*ft*) with a higher percentage found over steep hillsides and valley  
341 slopes (mean slope:  $21^0$ ) at a mean height of 493 m asl, associated with high roughness  
342 and severe landscape deformation.
- 343 • The Flysch-Schist allochthonous rocks (*f*) are rare, with their distribution characterized by  
344 geomorphometric classes 2, 3 and 4.
- 345 • The Ophiolites (*o*) have a small areal extent, mainly occurring between 493-617 m asl,  
346 characterized by the geomorphometric classes 4 and 5, with a large percentage found in  
347 plateaus and plains.
- 348 • The Carbonate allochthonous rocks (*K.m*) have small areal extent, mostly over low relief  
349 plains and valleys with minimal dissection.
- 350 • The Carbonate Pindos rocks (*K-E*) have a small areal extent (~3% total area coverage)  
351 and are found mainly in Rethymno and Herakleio districts. This tectonic nappe formation  
352 is characterized by the geomorphometric classes 3, 4 and 6, occurring between 371-838  
353 m asl, on gentle to steep slopes (mean:  $10^0$ - $22^0$ ), characterized by a very high degree of  
354 landscape deformation and high roughness.
- 355 • The Carbonate Tripolis rocks (*K.k*) (~15% total area coverage) are distributed over most  
356 of the geomorphometric classes (classes 2 to 7); the highest percentage (~22%) is found



357 at a mean height of 493 m asl with steep relief (mean:  $22^0$ ). This tectonic nappe formation  
358 is characterized by a high degree of landscape deformation and roughness.

359 • The Phyllite-Quartzite (*Ph-T*) (~12% total area coverage) is characterized by low to  
360 intermediate relief (mean: 208-838 m asl) and by geomorphometric classes 4 and 2;  
361 moderate to steep slopes (mean:  $17^0$ - $21^0$ ) and moderate to high roughness of hillsides and  
362 valley slopes.

363 • The Carbonate Tripali rocks (*T.br*) have a small areal extent (~3.6% total area coverage),  
364 mainly at high elevation (mean height: 838-1188 m asl) in geomorphometric classes 7  
365 and 6. It is characterized by steep slopes (mean:  $20^0$ - $22^0$ ), with a high degree of landscape  
366 deformation, dissection and roughness.

367 • The Plattenkalk nappe (*J-E*) (~16% total area coverage) is distributed over intermediate  
368 to high relief areas (mean: 493-1745 m asl), characterized by geomorphometric classes 4,  
369 6, 7 and 8. The Plattenkalk unit is characterized by steep slopes (mean:  $21^0$ - $24^0$ ), very  
370 high dissection, high roughness and V-shaped valleys associated with severe landscape  
371 deformation.

372

373 Crete corresponds to group *C* of the updated Koppen-Geiger climate classification: warm  
374 temperate climate (sub-classes *Cas*, *Cbs*, *Caf* and *Cbf*) (Table 3). *Cas* type (hot and dry summer)  
375 is the dominant climate type (Fig. 6). *Cas* is distributed over all the geomorphometric classes,  
376 with a high percentage characterized by low to intermediate relief, where *Q.al*, *Mk* and *K.k*  
377 formations exist, while the percentage of this climatic type decreases above ~800 m asl (Fig.  
378 8B). The *Caf* type (hot summer without dry season) is distributed over all the geomorphometric  
379 classes, but mainly characterizes the high relief mountainous blocks of Lefka Ori and Psiloritis

380 (Fig. 1). The *Cbs* type is found at mid to high altitudes (371-1188m asl) (Fig. 6), because of its  
381 climatic limits: the temperature of the hottest month is less than 22<sup>0</sup> C, but for 10 months per  
382 year the temperature remains more than 4<sup>0</sup> C (Fig. 8B).

383 Although the regional climatic classification approach of Kottke et al (2006) shows more  
384 details than the widely used Köppen-Geiger approach, its 0.5 degree (~50 x 50 km) spatial  
385 resolution still only characterizes the whole of Crete as having a *Cas* climate type. In this study a  
386 more detailed spatial resolution (0.6 x 0.6 km) of temperature and rainfall datasets was used, as  
387 determined by the EMERIC project (Sarris, 2007; Fassoulas et al., 2007). This produced a more  
388 detailed climatic classification of Crete which: revealed a wider range of climatic variation, with  
389 four climatic zones (*Cas*, *Cbs*, *Caf*, *Cbf*).

390 Based on the quantification of the geodiversity map, the highest *PRD* values were  
391 observed for Rethymno (~0.1) and Herakleio (~0.07) districts (Table 6), which have rock  
392 outcrops of relatively small areal extent and contain all the 12 geological formations. Large-area  
393 geological formations dominate Chania and Lasithi districts, which have the lowest *PRD* values  
394 (~0.04 and ~0.05 respectively) and contain 10 of the 12 geological formations (Table 6). Such  
395 observations are in accordance with the findings of Benito-Calvo et al. (2009), where an inverse  
396 correlation between *PRD* values and geological areas were observed. It indicates that *PRD* is not  
397 an appropriate index for the comparison of landscapes with variable areal extents, nor for  
398 evaluation of richness in complex, multi-lithology geological settings (Benito-Calvo et al.,  
399 2009).

400 The geodiversity of Crete was evaluated as *SHDI*= 4.32 or *SIDI*=0.976 (Table 6). For the  
401 individual districts, *SHDI* varies from 3.72 to 4.16 and the *SIDI* varies from 0.951 to 0.975  
402 (Table 6). Crete is characterized by very high diversity values, indicating the tectonically active

403 status in the region. It also has the highest *SHDI* and *SIDI* values in the geological classes (Table  
404 6), indicating high diversity and heterogeneous landscapes, due to the complex geological  
405 context across the island. Regarding the individual districts, the *SHDI* values are highest for  
406 Rethymno (~4.16), with Lasithi (~3.72) having the lowest value. The *SIDI* values are also the  
407 highest for Rethymno region, indicating the high diversity status, with the presence of all 12  
408 geological formations. That high diversity can be linked to the active Spili fault, a normal fault  
409 that extends onshore for ~20 km and traverses the central part of Crete with a NW-SE strike  
410 (Mouslopoulou, 2011). The Herakleio district has the lowest diversity values in  
411 geomorphometric classes (Table 6), with low relief alluvial deposits and gentle slopes. In  
412 general, western Crete (Chania and Rethymno districts) has higher diversity values in the  
413 geomorphometric classes than eastern Crete (Herakleio and Lasithi districts), reflecting the  
414 higher diversity and heterogeneity of the west, which experiences most of Crete's neotectonic  
415 activity, such as uplift and fault movement (Stiros, 1996; Shaw et al., 2008). The dominant  
416 geomorphometric classes that characterize western Crete indicate deep incised valleys, steep  
417 slopes, dissected terrain and high roughness, contrasting with the low relief alluvial deposits,  
418 gentle slopes, plains and low roughness of eastern Crete (Fig. 5 and Table 2).

419 Herakleio district has the lowest *SHEI* and *SIEI* values, indicating its low  
420 geomorphometric heterogeneity (Table 6). Lasithi has higher values of *SHEI* than Herakleio for  
421 the geodiversity map and geomorphometric classification, but the lowest *SHEI* values for the  
422 geological classification (Table 6). For the geological classification, Lasithi has a landscape  
423 where the distribution of area among the different geological formations becomes increasingly  
424 uneven, with *J-E*, *K.k* and *Mk* formations dominating. Rethymno district has the highest  
425 evenness indices values, with similar proportional relations as the respective diversity values.

426 Western Crete is characterized by maximum evenness, relative to eastern Crete, with the  
427 variation among the evenness indices being quite discrete (Table 6). Such variation could be  
428 linked to the extensive area of low relief plains that characterize eastern Crete, relative to the  
429 more complex heterogeneous terrain of western Crete, with its higher degree of neotectonic  
430 activity.

431 To quantify the landscape shape characteristics, the spatial pattern indices of *SHAPE*,  
432 *CIRCLE* and *PAFRAC* were calculated (Table 6). High values for *SHAPE* were found in  
433 Rethymno district where the patch shape becomes more irregular, due to dissected terrain with  
434 V-shaped incised valleys and steep slopes, indicating severe landscape deformation. Lower  
435 *SHAPE* values are observed in Lasithi district, where more regular patches correspond to lower  
436 landscape deformation and extensive low relief plains (Table 6). *CIRCLE* values are higher for  
437 Chania and Rethymno, with elongated landscape patches where elongation can be associated  
438 with active tectonics. High values of *PAFRAC* occur on the geological classes observed in  
439 western Crete, indicating the complex geodiversity of the region, with highly convoluted  
440 perimeters relative to the lower values that characterize Herakleio and Lasithi (Table 6). In the  
441 geodiversity map there are a few small variations with simple shape perimeters, highlighted by  
442 the lowest values of the index in Herakleio district (Table 6). In the geomorphometric  
443 classification, the smallest patch shape complexity is observed in Lasithi district, with higher  
444 complexity in Herakleio linked to the diverse transition from low relief plains to high relief steep  
445 mountain blocks (e.g. Psiloritis) and the southern coastline, where active faults in the Messara  
446 basin form rough terrain (Mouslopoulou, 2011) (Table 6).

447 To characterize landscape fragmentation, the indices of *PD* and *PROX* were evaluated  
448 (Table 6). Rethymno and Chania districts are characterized by high *PD* values on the

449 geodiversity map, indicating the complex geodiversity for western Crete. Lasithi district has very  
450 high *PD* values for the geological classification, which indicates a diverse geological pattern  
451 with the presence of all 12 geological formations. Herakleio district has the highest *PD* values  
452 regarding the geomorphometric classes, but the lowest for the terrain and geological  
453 classifications (Table 6). In this case, Herakleio district has uniform terrain and landscape  
454 patterns, from large areas of low relief plains on Cenozoic formations, contrasting with its  
455 southern coast, where most of the geomorphological classes are present in rough terrain with  
456 active faults (Mouslopoulou, 2011). Low *PROX* values for all classifications characterize  
457 Rethymno district, indicating high fragmentation (Table 6). Herakleio district has the highest  
458 *PROX* values, indicating homogenous patches which are less fragmented in distribution.

## 459 **5. Discussion**

460 This study has assessed the geodiversity of Crete by quantifying its terrain characteristics,  
461 based on geomorphological, geological and climatic information. The methodology followed the  
462 approach of Benito-Calvo et al. (2009), with a few modifications, notably:

463 i) the geomorphological classification consisted of various geomorphometric indices to  
464 highlight the geomorphological, hydrological and morphotectonic context;

465 ii) the climatic classification was based on the Kottek et al (2006) approach, but used a  
466 higher-resolution grid (0.6 x 0.6 km) which revealed a larger variation of climatic zones;

467 iii) the geodiversity quantification was based on a higher number of spatial pattern  
468 indices: as well as landscape evenness and diversity, we also examined fragmentation, shapes  
469 and their linkages.

470 The distribution of nappes across Crete is well recorded (e.g. Seidel et al., 1982;  
471 Fassoulas et al., 1994) but their geomorphological characteristics are less well known. The

472 geomorphometric classification derived in this study determined the geomorphological context  
473 of those geological units. Based on the topographic, permeability and rock strength  
474 characteristics of the geological units, the nappes were characterized in terms of their roughness,  
475 dissection, landscape deformation, rock resistance to erosion and steepness. The erosion-  
476 resistant nappes (*J-E*, *T-Br*, *Ph-T*, *K.k* and *K-E* formations) form high relief regions,  
477 characterized by moderate to high roughness and dissection with V-shaped valleys, low moisture  
478 accumulation (lack of fine drainage network) and interlinkage with tectonic activity. The post-  
479 Alpine rocks, such as the weak *Q.al* and *Mk* formations, are found in low relief regions with less  
480 dissected plains and valleys, characterized by high moisture accumulation, fine drainage texture  
481 and smooth-relief landscapes that are devoid of features that indicate abrupt/tectonic  
482 deformation, such as fault scarps.

483         The Benito-Calvo et al. (2009) study quantified geodiversity based on diversity and  
484 evenness determinations. In this study, additional spatial pattern indices were considered for  
485 quantifying geodiversity. This has produced a better understanding of the fragmentation and  
486 shape characteristics of landscape patterns across Crete, by evaluating the degree of homogeneity  
487 or heterogeneity, the distributed fragmentation (or irregularity) of the landscape and link to  
488 neotectonic activity.

489         The methodology presented in this study can be useful for decision makers when  
490 evaluating a region's geological heritage, planning the management of natural resources or  
491 designating areas for conservation, for instance. Crete is a 'natural laboratory' with a rich  
492 geological heritage and diverse terrain. It has a dynamic landscape with high neotectonic activity  
493 interacting with weathering and erosion to shape its terrain and landscape structure. In the  
494 context of climate change, population pressure/urbanization and degradation of natural resources,

495 the quantification of geodiversity - facilitated by geoinformatics - provides valuable data and  
496 maps for planners, decision-makers and policy-makers (Kostrzewski, 2011).

497

## 498 **6. Conclusions**

499 During the last decade the assessment of geodiversity has become a major research topic  
500 of the geoinformatic research community with landscape indices providing a powerful approach.  
501 The evaluation of geomorphometric, geological and climatic data sets can be integrated using  
502 low-cost GIS techniques, highlighting information within the interlinked geographic data. Such  
503 data integration, analysis and mapping can produce a geodiversity map which can highlight and  
504 categorize the characteristic information. The geodiversity map, along with landscape richness,  
505 evenness, fragmentation and shape irregularity, were examined via the calculated landscape  
506 indices. Those indices highlighted the correlations between the areal extent of lithologies for  
507 each district across Crete, with larger lithological units dominating Chania and Lasithi districts.  
508 The outcome showed that Rethymno district is characterized by maximum richness and  
509 evenness, while high diversity and heterogeneous landscapes characterized Chania district.  
510 Western Crete is characterized by complex geodiversity with a more irregular, elongated and  
511 fragmented landscape pattern, relative to the eastern part of the island. The overall extracted  
512 data, gives important information for quantifying geodiversity across Crete. The methodology  
513 presented provides useful information for research into landscape composition and specific  
514 geodiversity concerns, such as the aesthetic value of one landscape type over another. This can  
515 be especially useful when delineating the boundaries of national parks and other protected areas.

516

517

## Acknowledgements

518 The work was supported by the project POLITEIA of Action KRIPIS of the General Secretary  
519 for Research and Technology under the framework of the operational programme  
520 “Competitiveness and Entrepreneurship – NSRF 2017-2013”.

521

522

## References

- 523 Anderson, M. G. and Kneale, P. E. (1982): The influence of low-angled topography on hillslope soil-  
524 water convergence and stream discharge. *Journal Hydrol.*, 57, pp 65 – 80.
- 525 Argyriou, A.V., Teeuw, R.M., Rust, D., Sarris, A., 2016. GIS multi-criteria decision analysis for  
526 assessment and mapping of neotectonic landscape deformation: A case study from Crete.  
527 *Geomorphology*. Vol. 253, pp. 262-274.
- 528 Aubouin, J. and Dercourt, J., 1970. Sur la geologie de l’ Egee: regard sur le Dodecanese meridional  
529 (Kassos, Karpathos, Rhodes). *Bull. Soc. Géol. France* 7, XII, pp. 455–472.
- 530 Awasthi, K. D., Sitaula, B. K., Singh, R. B. R., Bajacharaya, M., 2002. Land-use change in two Nepalese  
531 watersheds: GIS and geomorphometric analysis. *Land Degrad. Develop.* 13, pp 495–513.
- 532 Bagyaraj, M. and Gurugnanam, B., 2011. Significance of Morphometry Studies, Soil Characteristics,  
533 Erosion Phenomena and Landform Processes Using Remote Sensing and GIS for Kodaikanal Hills, A  
534 Global Biodiversity Hotpot in Western Ghats, Dindigul District, Tamil Nadu, South India. Research  
535 *Journal of Environmental and Earth Sciences* 3(3), pp 221-233.
- 536 Baumann, A., Best, G., Gwosdz, W., Wachendorf, H., 1976. The nappe pile of eastern Crete.  
537 *Tectonophysics*, 30, pp. 33-40.
- 538 Benito-Calvo, A., Perez-Gonzalez, A., Magri, O., Mesa, P., 2009. Assessing regional geodiversity: the  
539 Iberian Peninsula. *Earth Surf. Process. Landforms* 34, pp 1433–1445.
- 540 Berger, K. and Entekhabi, D.: Basin Hydrologic Response Relations to Distributed Physiographic  
541 Descriptors and Climate, *J. Hydrol.*, 247, pp 169–182.
- 542 Berry, J. K., 2002. Use surface area for realistic calculations. *Geoworld* 15(9), pp 20–21.
- 543 Beven, K.J and Kirkby, M.J (1979): A physically based, variable contributing area model of basin  
544 hydrology. *Hydrol. Sci.Bull.*, 24, pp 43-69.
- 545 Bruschi, VM. 2007. Desarrollo de una metodología para la caracterización, evaluación y gestión de los  
546 recursos de la geodiversidad, PhD Thesis, Universidad de Cantabria, Santander; pp 355.
- 547 Carcavilla L., Duran J.J., Lopez-Martinez J., 2008. Geodiversidad: concepto y relacion con el patrimonio  
548 geologico. *Geo-Temas* 10, pp. 1299–1303 (in spanish with english abstract).



- 549 Chatzaras, V., Xypolias, P., and Doutsos, T., 2006. Exhumation of high pressure rocks under continuous  
550 compression: a working hypothesis for southern Hellenides (central Crete, Greece). *Geological Magazine*,  
551 v. 143, no. 6, pp. 859-876.
- 552 Chorley, R.J., Schumm, S.A., Sugden, D.E., 1984. *Geomorphology*. Methuen & Co: London; pp. 605.
- 553 Christian, C.S., and Stewart, G.A., 1952. Summary of general report on survey of Katherine-Darwin  
554 Region, 1946. Land Research Series, 1, CSIRO, Australia, pp 24.
- 555 Ciccacci, S., De Rita, D., Fredi, P., 1988. Geomorfologia quantitativa e morfotettonica dell'area di  
556 Morlupo-Castelnuovo di Porto nei Monti Sabatini (Lazio). *Supplemento di Geografia Fisica e Dinamica*  
557 *Quaternaria I*, pp 197-206.
- 558 Ciotoli, G., Della Seta, M., Del Monte, M., Fredi, P., Lombardi, S., Lupia Palmieri, E., Pugliese, F., 2003.  
559 Morphological and geochemical evidence of neotectonics in the volcanic area of Monti Vulsini  
560 (Latium,Italy). *Quaternary International* 101–102, pp 103–113.
- 561 Clarke, J.I. 1966. Morphometry from maps. In: Dury, G.H. (ed) *Essays in Geomorphology*. London,  
562 Heinemann, pp 235- 274.
- 563 Conacher, A.J. and Dalrymple, J.B., 1977. The Nine-unit Landsurface Model: an approach to  
564 pedogeomorphic research. *Geoderma*, 18, pp 1-154.
- 565 Currado, C. and Fredi, P. (2000): Morphometric parameters of drainage basins and morphotectonic  
566 setting of eastern Abruzzo. *Memorie della Società Geologica Italiana*, 55, pp 411-419.
- 567 Della Seta, M., Del Monte, M., Fredi, P., Lupia Palmieri, E., 2004. Quantitative morphotectonic analysis  
568 as a tool for detecting deformation patterns in soft-rock terrains: a case study from the southern Marches,  
569 Italy. *Géomorphologie: relief, processus, environnement*, n 4, pp 267-284.
- 570 ESRI, 2003. ArcGis Desktop Help, in ArcMap utility.
- 571 Evans, I.S. 1972. General geomorphometry, derivatives of altitude, and descriptive statistics. In: Chorley,  
572 R.J. (ed) *Spatial Analysis in Geomorphology*. London, Methuen, pp 17-90.
- 573 Fassoulas, C., Kiliyas, A. and Mountrakis, D., 1994. Postnappe stacking extension and exhumation of  
574 high-pressure/low temperature rocks in the island of Crete, Greece. *Tectonics*,13, pp. 127-138.
- 575 Fassoulas, Ch., Georgila, K., Sarris, A., Kokkinaki, M., 2007. Geohazard risk assessment based on the  
576 evaluation of Cretan faults, Crete-Greece. *The 6th International Symposium on Eastern Mediterranean*  
577 *Geology & The 9th International Conference of Jordanian Geologists Association*, Amman, Jordan.
- 578 Fytrolakis, N., 1980. The geological structure of Crete: Problems, observations, and conclusions. Habil.  
579 Thesis, Nat. Techn. Univ. Athens, pp.143.
- 580 García-Tortosa, F.J., Alfaro, P., Galindo-Zaldívar, J., Gibert, L., López-Garrido, A.C., Sanz de Galdeano,  
581 C., Ureña, M., 2008. Geomorphologic evidence of the active Baza Fault (Betic Cordillera, South Spain).  
582 *Geomorphology* 97, pp 374–391.
- 583 Geiger, R., 1954. Klassifikationen der Klimate nach W. Köppen. In:Landolf-Börnstein:Zahlenwerte und  
584 Funktionen aus Physik, Chemie, Astronomie, Geophysik und Technik, (alte Serie), Vol. 3. Springer,  
585 Berlin, pp 603–607.

- 586 Gordon, J.E., Barron, H.F., Hansom, J.D., Thomas, M.F., 2012. Engaging with geodiversity—why it  
587 matters. *Proc Geol Assoc*, 123, pp. 1–6.
- 588 Gray, M. 2004. Geodiversity: Valuing and Conserving Abiotic Nature. John Wiley & Sons: Chichester;  
589 pp 434.
- 590 Hack, J., 1973. Stream profile analysis and stream gradient index, *U. S. Geol. Surv. J. Res.* 1, pp. 421-  
591 429.
- 592 Hjerdt, K.N, McDonell, J.J, Seibert, J., Rodhe, A., 2004. A new topographic index to quantify downslope  
593 controls on local drainage. *Water Resources Research*, Vol. 40, W05602, pp 1-6.
- 594 Hjort, J. and Luoto, M., 2010. Geodiversity of high-latitude landscapes in northern Finland.  
595 *Geomorphology*, 115(1–2), pp. 109–116.
- 596 Horton, R.E., 1945. Erosional development of streams and their drainage basins; hydrophysical approach  
597 to quantitative morphology. *Geol. Soc. Am. Bull.* 56, pp. 275–370.
- 598 IGME, 1971. Geological Map of Greece, western Crete sheets. Athens:  
599 Institute of Geology and Mineral Exploration. Scale: 1:50,000.
- 600 Jamieson, S.S.R., Sinclair, H.D., Kirstein, L.A., Purves, R.S., 2004. Tectonic forcing of longitudinal  
601 valleys in the Himalaya: morphological analysis of the Ladakh Batholith, North India. *Geomorphology*  
602 58, pp 49-65.
- 603 Jenness, J.S., 2004. Calculating landscape surface area from digital elevation models. *Wildfire Society*  
604 *Bulletin*, 32 (3), pp. 829-839.
- 605 Keller, E.A., 1986. Investigation of active tectonics: Use of surficial earth processes. In: Wallace, R.E.  
606 (Ed.), *Active Tectonics. Studies in Geophysics*. The National Academies Press, Washington, DC, pp 136–  
607 147.
- 608 Keller, E.A. and Pinter, N., 1996. *Active Tectonics (Earthquakes, Uplift and Landscape)*. Prentice-Hall  
609 Inc., New Jersey, pp 339.
- 610 Keller, E. A. and Pinter, N., 2002. *Active Tectonics: Earthquakes and Landscape*. Second Edition.  
611 Prentice-Hall: Upper Saddle River, New Jersey, pp 362.
- 612 Kelletat, D., 1996. Perspectives in coastal geomorphology of western Crete, Greece. *Zeitschrift für*  
613 *Geomorphologie N. F.*, Supplement Band 102, pp 1-19.
- 614 Köppen, W., 1936. Das geographische System der Klimate. In: Köppen W, Geiger R (eds) *Handbuch der*  
615 *Klimato - logie*. Gebrüder Borntraeger, Berlin, pp 1–44.
- 616 Kostrzewski, A., 2011. The role of relief geodiversity in geomorphology. *Geographia Polonica*, 84,  
617 special issue 2, pp. 69-74.
- 618 Kottek, M., Grieser, J., Beck, C., Rudolf, B., Rubel, F., 2006. World map of the Köppen-Geiger climate  
619 classification updated, *Meteorol. Z.*, 15, pp 259–263.
- 620 Kouli, M., Vallianatos, F., Soupios, P., Alexakis, D., 2007. GIS-based morphometric analysis of two  
621 major watersheds, western Crete, Greece, *Journal of Environmental Hydrology* 15, pp 1-17.

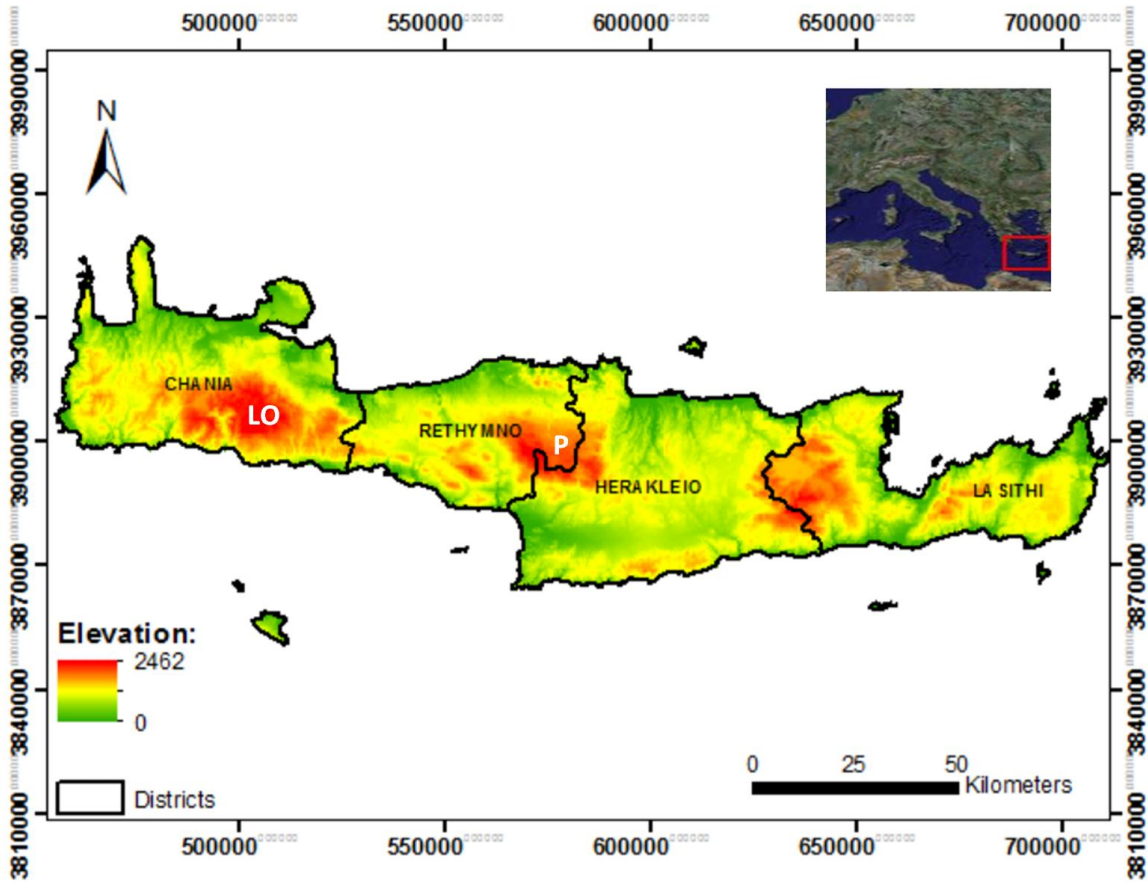
- 622 Kozłowski S. 2004. Geodiversity. The concept and scope of geodiversity. *Przegląd Geologiczny* 52(8/2),  
623 pp 833–837.
- 624 Leopold, L.B., 1969. Quantative comparison of some aesthetic factors among rivers. *USGS Circular*, 620,  
625 pp 16.
- 626 Luo W., 1998. Hypsometric analysis with a Geographic Information System. *Computers & Geosciences*  
627 Vol. 24, No. 8, pp 815-821.
- 628 Maidment, D., 2002. Arc Hydro: GIS for Water Resources. Redlands, CA, USA: ESRI Press, Volume 1,  
629 203pp.
- 630 Meulenkamp, J.E., Dermitzakis, M.D., Georgiades-Dikeoulia, E., Jonkers, H.A. & Boger, H., 1979.  
631 Field guide to the Neogene of Crete. Publ. of the Department of Geology and Paleontology, Univ. of  
632 Athens, ser. A, no32, pp. 32.
- 633 McAdoo, B.G., Capone, M.K., and Minder, J., 2004. Seafloor geomorphology of convergent margins:  
634 Implications for Cascadia seismic hazard. *Tectonics*, vol. 23, TC6008, pp. 1-15.
- 635 McGarigal, K., Cushman, S.A., Neel, M.C., Ene, E., 2002. FRAGSTATS: Spatial Pattern Analysis  
636 Program for Categorical Maps. Computer software program produced by the authors at the University of  
637 Massachusetts: Amherst, pp 51.
- 638 Mesa, L. M., 2006. Morphometric analysis of a subtropical Andean basin (Tucuman, Argentina). *Environ*  
639 *Geol* (2006) 50, pp 1235–1242.
- 640 Migon, P., Kasprzak, M., Traczyk, A., 2013. How high-resolution DEM based on airborne LIDAR helped  
641 to reinterpret landforms—examples from the Sudetes. SW Poland. *Landform Anal.* 22, pp. 89-101.
- 642 Mouslopoulou, V., Moraetis, D., and Fassoulas, Ch., 2011. Identifying past earthquakes on carbonate  
643 faults: Advances and limitations of the ‘Rare Earth Element’ method based on analysis of the Spili Fault,  
644 Crete, Greece. *Earth and Planetary Science Letters*, 309, pp. 45-55.
- 645 Mukhopadhyay, S.C., 1984. The Thisa Basin – A Study in Fluvial Geomorphology, K.P. BanchiandCo.,  
646 Calcutta, pp 308.
- 647 Nieto LM. 2001. Geodiversity: proposal of an integrative definition. *Boletín Geológico y Minero*, 112(2),  
648 pp 3–12.
- 649 Ollier, C.D., Lawrance, C.J., Webster, R., Beckett, P.H.T., 1969. *The Land Systems of Uganda*. Report  
650 959, M.E.X.E., Christchurch, UK, pp 234.
- 651 Ozdemir, H. and Bird, D., 2009. Evaluation of morphometric parameters of drainage networks derived  
652 from topographic maps and DEM in point of floods. *Environmental Geology*. Volume 56, Issue 7, pp  
653 1405-1415.
- 654 Panizza, M. and Piacente S., 2008. La geodiversità e una sua applicazione nel territorio emiliano. *Il*  
655 *Geologo dell'Emilia-Romagna* 29, pp 35–37.
- 656 Papanikolaou, D. & Vassilakis, E., 2009. Thrust faults and extensional detachment faults in Cretan  
657 tectono-stratigraphy: Implications for Middle Miocene extension. *Tectonophysics*, Vol. 488, pp. 233-  
658 247.

- 659 Papastamatiou, J. & Reichel, M., 1956. Sur l' age des phyllades de l' ile de Crete. *Ecl. Geol. Helv.* 49, pp.  
660 147.
- 661 Papastamatiou, J., Vetoulis, D., Bornovas, J., Christodoulou, G. & Katsikatos, G., 1959. Geologische  
662 Karte von Kreta (1:50.000) Blatt Ziros. *Inst. Geol. Subsurf. Res.*, Athens.
- 663 Papazachos, B.C. and Comninakis, P.E., 1978. Deep structure and tectonics of the Eastern Mediterranean.  
664 *Tectonophysics*, 33, pp 285-296.
- 665 Pareta, K. and Pareta, U., 2011. Quantitative morphometric analysis of a watershed of Yamuna basin,  
666 India using ASTER (DEM) data and GIS. *International Journal of Geomatics and Geosciences*, vol. 2,  
667 no1, pp. 248-269.
- 668 Parks, K.E., Mulligan, M., 2010. On the relationship between a resource based measure of geodiversity  
669 and broad scale biodiversity patterns. *Biodiversity and Conservation*, 19, pp. 2751–2766.
- 670 Pereira, D.I., Pereira, P., Brilha, J., Santos, L., 2013. Geodiversity assessment of Parana state (Brazil): an  
671 innovative approach. *Environmental Management*, pp. 1-12.
- 672 Pike, R.J. and Wilson, S.E., 1971. Elevation-relief ratio, hypsometric integral, and geomorphic area-  
673 altitude analysis. *Geological Society of America Bulletin*, v.82, pp 1079-1084.
- 674 Pirazzoli, P.A., Laborel, J., Stiros, S.C., 1996. Earthquake clustering in the Eastern Mediterranean  
675 during historical times. *J. Geophys. Res.*, 101 (B3), pp. 6083–6097.
- 676 Pirazzoli, P.A., 2005. A review of possible eustatic, isostatic and tectonic contributions in eight late-  
677 Holocene relative sea-level histories from the Mediterranean area. *Quaternary Science Reviews* 24, pp  
678 1989-2001.
- 679 Rawat P., 2013. GIS Modeling on Mountain Geodiversity and its Hydrological Responses: in View of  
680 Climate Change. Book by LAP LAMBERT Academic Publishing (May 1, 2013), pp 188.
- 681 Reddy, G. P. Obi, Maji, A. K., Gajbhiye, K. S., 2004. Drainage morphometry and its influence on  
682 landform characteristics in a basaltic terrain, Central India – a remote sensing and GIS approach.  
683 *International Journal of Applied Earth Observation and Geoinformation*, 6, pp 1–16.
- 684 Renz, C., 1955. Die vom eogene Stratigraphie der normaledimentären Formationen Griechenlands, *Inst.*  
685 *Geol. Subsurf. Res.*, pp. 637.
- 686 Rowberry, M.D., 2012. A comparison of three terrain parameters that may be used to identify denudation  
687 surfaces within a GIS: a case study from Wales, United Kingdom. *Computers & Geosciences*, 43, pp 147-  
688 158.
- 689 Ruban, D., 2010. Quantification of geodiversity and its loss. *Proc Geol Assoc*, 121, pp. 326–333
- 690 Sarris A., Karakoudis S., Bidaki X., Soupios P., 2005. Study of the Morphological Attributes of Crete  
691 through the Use of Remote Sensing Techniques. *IASME Trans*, Issue 6, Vol. 2, pp 1043-1051.
- 692 Sarris, A., Fassoulas, Ch., Karathanasi, V., Mertikas, ST., Pprintsos, St., Savvaidis., A., Soupios, P.,  
693 Vallianatos, F., 2006. A Web-GIS Portal of the Natural Resources of the island of Crete. ESRI 21<sup>st</sup>  
694 European Conference on ArcGIS Users, Athens, November 7-8, 2006.

- 695 Sarris, A., 2007. Management of landscape & natural resources through remote sensing & GIS. *The*  
696 *International Society for Optical Engineering*, SPIE Newsroom.
- 697 Sen, P. K., 1993. Geomorphological analysis of drainage basins. The University of Burdwan, Burdwan.
- 698 Seidel, E., 1971. Die Pindos-serie in Westkreta , auf der insel Gavdos und im Kedros-Gebiet  
699 (Mittelkreta). *N. Jb. Geol. Palaont. Abh.*, 137, pp. 443-460.
- 700 Seidel, E., Kreuzer, H. and Harre, W., 1982. A Late Oligocene/Early Miocene high pressure belt in the  
701 external Hellenides. *Geol. Jahrb.*, E 23, pp. 165-206.
- 702 Serrano, E. and Flaño, P., 2007. Geodiversity: concept, assessment and territorial application. The case of  
703 Tiermes-Caracena. *Boletín de la AGE* 45, pp 389–393.
- 704 Shannon, C.E. and Weaver, W., 1949. The Mathematical Theory of Communication. University of  
705 Illinois Press, Urbana.
- 706 Sharples, C., 2002. Concepts and principles of geo-conservation. Tasmanian Parks and Wildlife Service  
707 web.
- 708 Shaw, B., Ambraseys, N. N., England, P. C., Floyd, M. A., Gorman, G. J., Higham, T. F. G., Jackson, J.  
709 A., Nocquet, J. M., Pain, C. C., Piggott, M. D., 2008. Eastern Mediterranean tectonics and tsunami hazard  
710 inferred from the AD 365 earthquake: *Nature Geoscience* 1, pp 268-276.
- 711 Simpson, E. H., 1949. Measurement of diversity. *Nature* 163:688.
- 712 Singh, S. and Dubey, A., 1994. Geoenvironmental Planning of Watershed in India, Chug publications,  
713 Allahabad, India, pp 28-69.
- 714 Sorensen, R., Zinko, U., Seibert, J., 2005. On the calculation of the topographic wetness index: evaluation  
715 of different methods based on field observations. *Hydrology and Earth System Sciences Discussions* 2, pp  
716 1807-1834.
- 717 Soupios, P., Sarris, A., Papadakis, G., Papazoglou, M., Vallianatos, F., Makris, J., 2005. Compilation of a  
718 Relational Digital Database for Monitoring and Management of Geo-Environmental Data in Crete  
719 Region. Proceedings of the 2005 Iasme/Wseas International Conference on Engineering Education,  
720 Vouliagmeni, Athens, Greece, July 8-10, 2005, pp 423-430.
- 721 Spellerberg, I. and Fedor, P.J., 2003. A tribute to Claude Shannon (1916– 2001) and a plea for more  
722 rigorous use of species richness, species diversity and the ‘Shannon–Wiener’ Index. *Global Ecology &*  
723 *Biogeography* 12, pp 177–179.
- 724 Sreedevi, P.D., Owais, S., Khan, H.H., Ahmed, S., 2009. Morphometric Analysis of a watershed of South  
725 India using SRTM Data and GIS, *Journal Geological Society of India*, vol. 73, pp 543-552.
- 726 Stavi, I., Shem-To, R., Chocron, M., Yizhaq, H., 2015. Geodiversity, self-organization, and health of  
727 three-phase semi-arid rangeland ecosystems, in the Israeli Negev. *Geomorphology*, 234, pp. 11-18.
- 728 Stiros, S., 1996. Late Holocene relative sea level changes in SW Crete evidence of an unusual earthquake  
729 cycle. *Annali di Geofisica*, 3, pp. 677-687.
- 730 Stiros, S., 2001. The AD 365 Crete earthquake and possible seismic clustering during the fourth to sixth  
731 centuries AD in the Eastern Mediterranean: a review of historical and archaeological data. *J. Struct.*  
732 *Geol.*, 23, pp. 545-562.

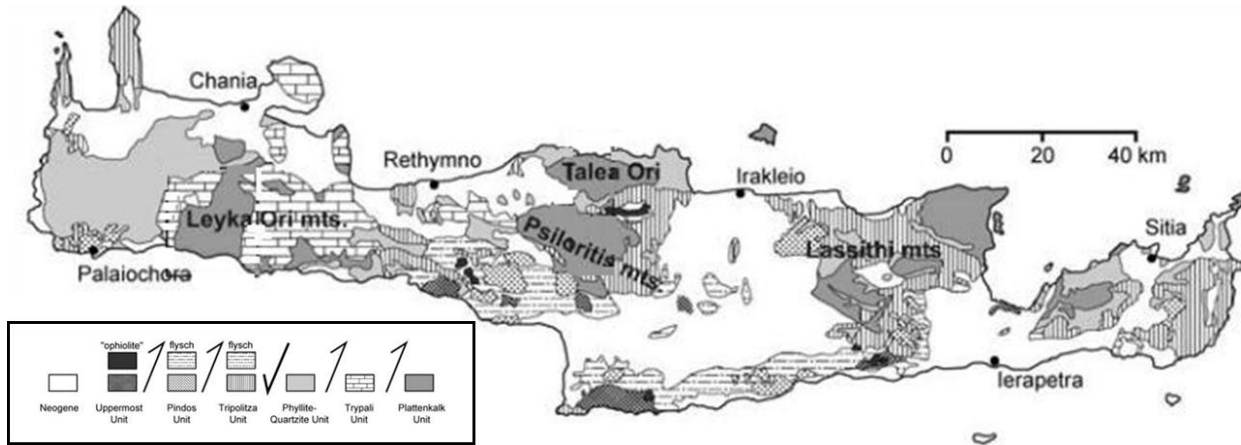
- 733 Strahler, A.N., 1952. Hypsometric (area–altitude) analysis of erosional topography. *Geological Society of*  
734 *America Bulletin* 63, pp 1117–1142.
- 735 Strahler, A.N., 1958. Dimensional analysis applied to fluvial eroded landforms. *Geological Society of*  
736 *America Bulletin* 69, pp 279-299.
- 737 Strahler, A.N., 1964. Quantitative geomorphology of basins and channel networks. In: Chow, V.T. (Ed.),  
738 *Handbook of Applied Hydrology*. Mcgraw Hill Book Company, New York.
- 739 Tarboton, D.C., Bras, R.L., Rodriguea-Iturbe, I., 1988. The fractal nature of river networks. *Water*  
740 *Resources Research* 24 (8), pp. 1317–1322.
- 741 Toudeshki, V.H. and Arian, M., 2011. Morphotectonic Analysis in the Ghezel Ozan River Basin, NW  
742 Iran. *Journal of Geography and Geology* 3, pp 258-265.
- 743 Troiani, F. and Della Seta, M., 2008. The use of the Stream Length–Gradient index in morphotectonic  
744 analysis of small catchments: A case study from Central Italy. *Geomorphology* 102, pp 159-168.
- 745 Tucker, G.E. and Bras, R.L., 1998. Hillslope processes, drainage density, and landscape morphology.  
746 *Water Resources Research*, Vol. 34, No. 10, pp 2751–2764.
- 747 Verstappen, H.T., 1983. *Applied geomorphology*. ITC, Enschede.
- 748 Zavoianu, I., 1985. Morphometry of Drainage Basins. *Developments in Water Science*, 20, pp. 238.
- 749
- 750 Figures and Tables:

751



752

753 **Fig. 1.** The island of Crete, with red tones highlighting mountainous relief (LO: Lefka Ori; P: Psiloritis).



Post Alpine Rocks	Quaternary		Alluvial and marine deposits Marls, clays, conglomerates, limestones	
	Neogene			
Alpine and Pre-Alpine Rocks	Upper nappes	LP-HT metamorphosed	Uppermost nappes Schists, oceanic pillow basalts	
		unmetamorphosed	Pindos nappe Limestones, shales and calc-breccias	
		LP-LT metamorphosed	Tripoli nappe Carbonates, dolomites and flysch	
	Lower nappes	Major thrust fault		Phyllite and quartzites
		HP-LT metamorphosed	Phyllite-Quartzite nappe	
Trypali nappe			Limestones, mudstones, recrystallized conglomerates	
		Plattenkalk nappe	Dolomites, dolomitic limestones.	

\*LP: low pressure; HP: high pressure; HT: high temperature; LT: low temperature

754

755 **Fig. 2.** The distribution of the major nappe piles formation across Crete (modified from Fassoulas, 1994 and Chatzaras, 2006).

756

757

758

759

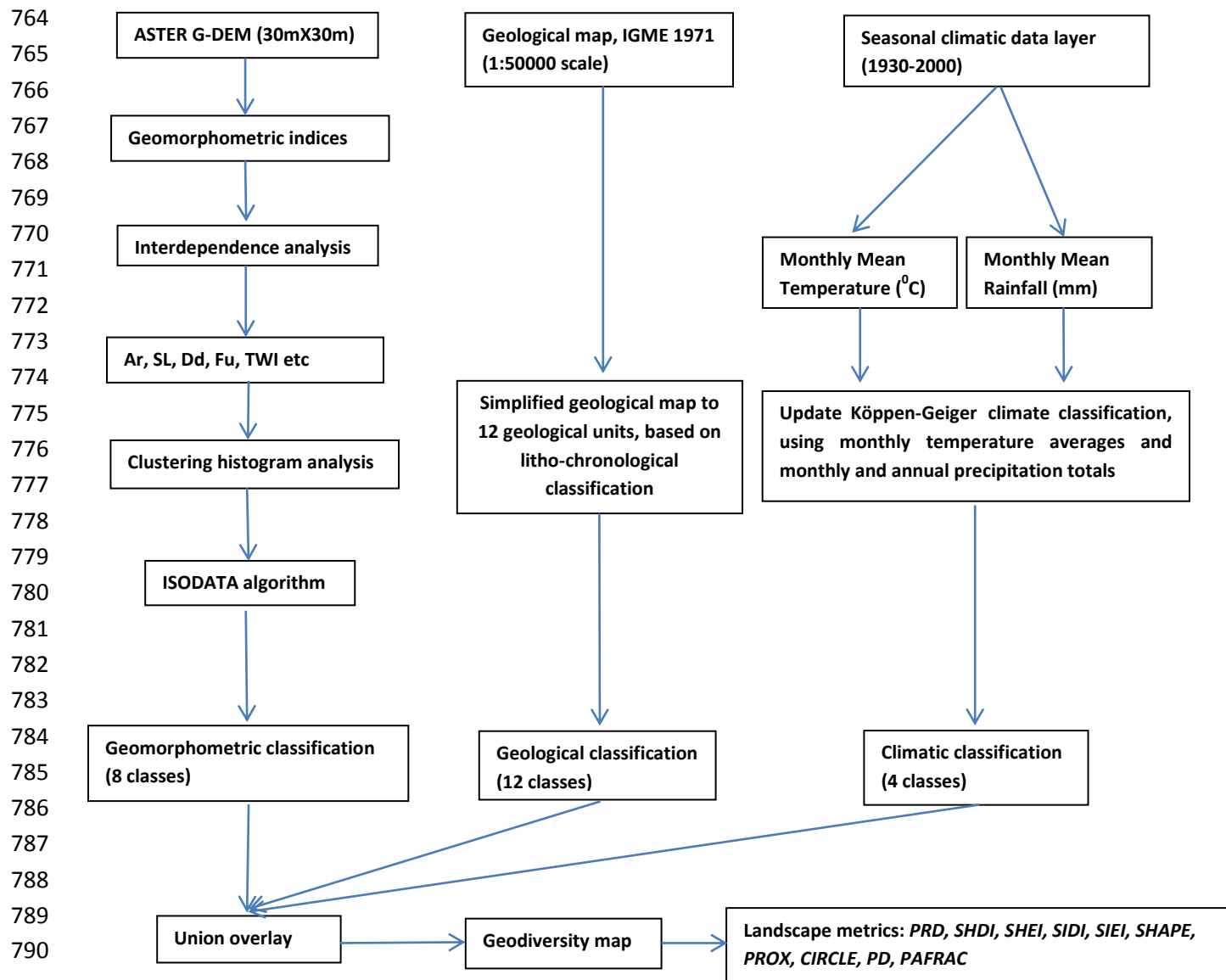
760

761

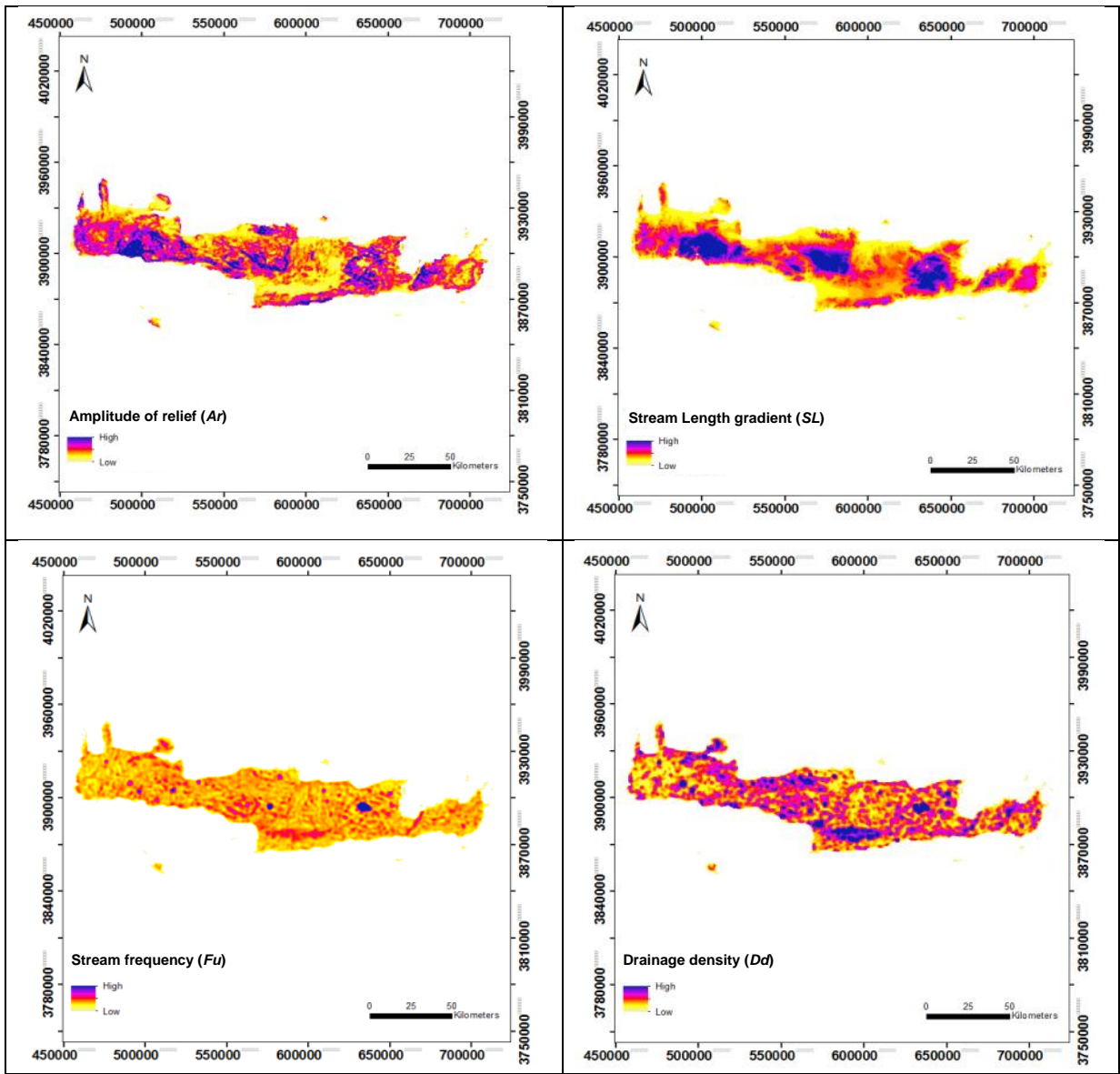
762

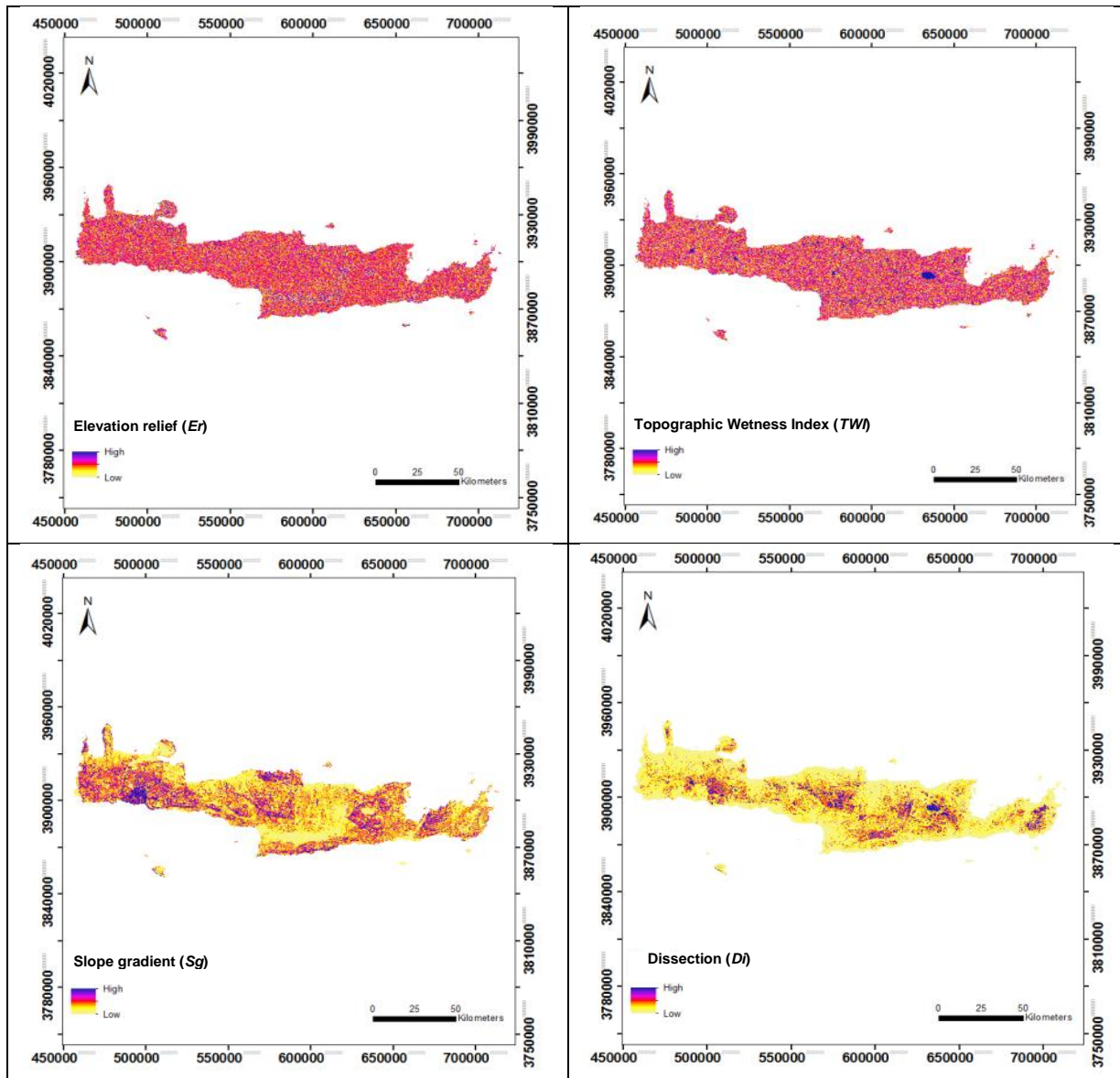
763

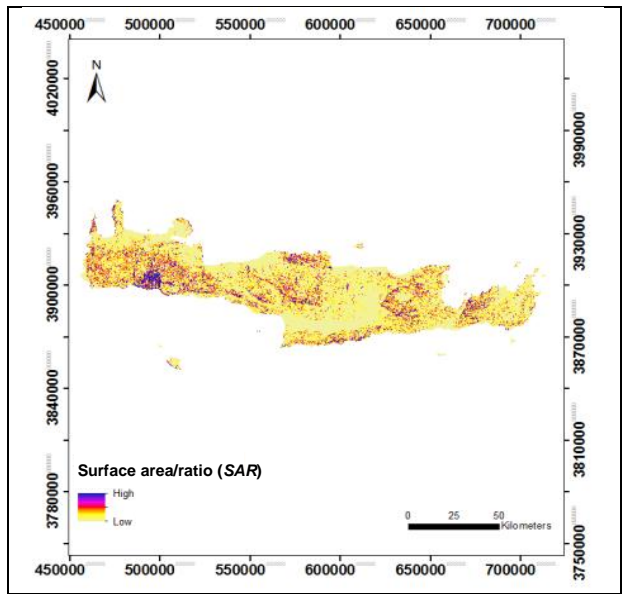




791 **Fig. 3.** Methodological framework used to assess regional geodiversity in Crete.







792

793 **Fig. 4.** The thematic maps of the nine geomorphometric indices that were considered during the geomorphometric classification.

794

795

796

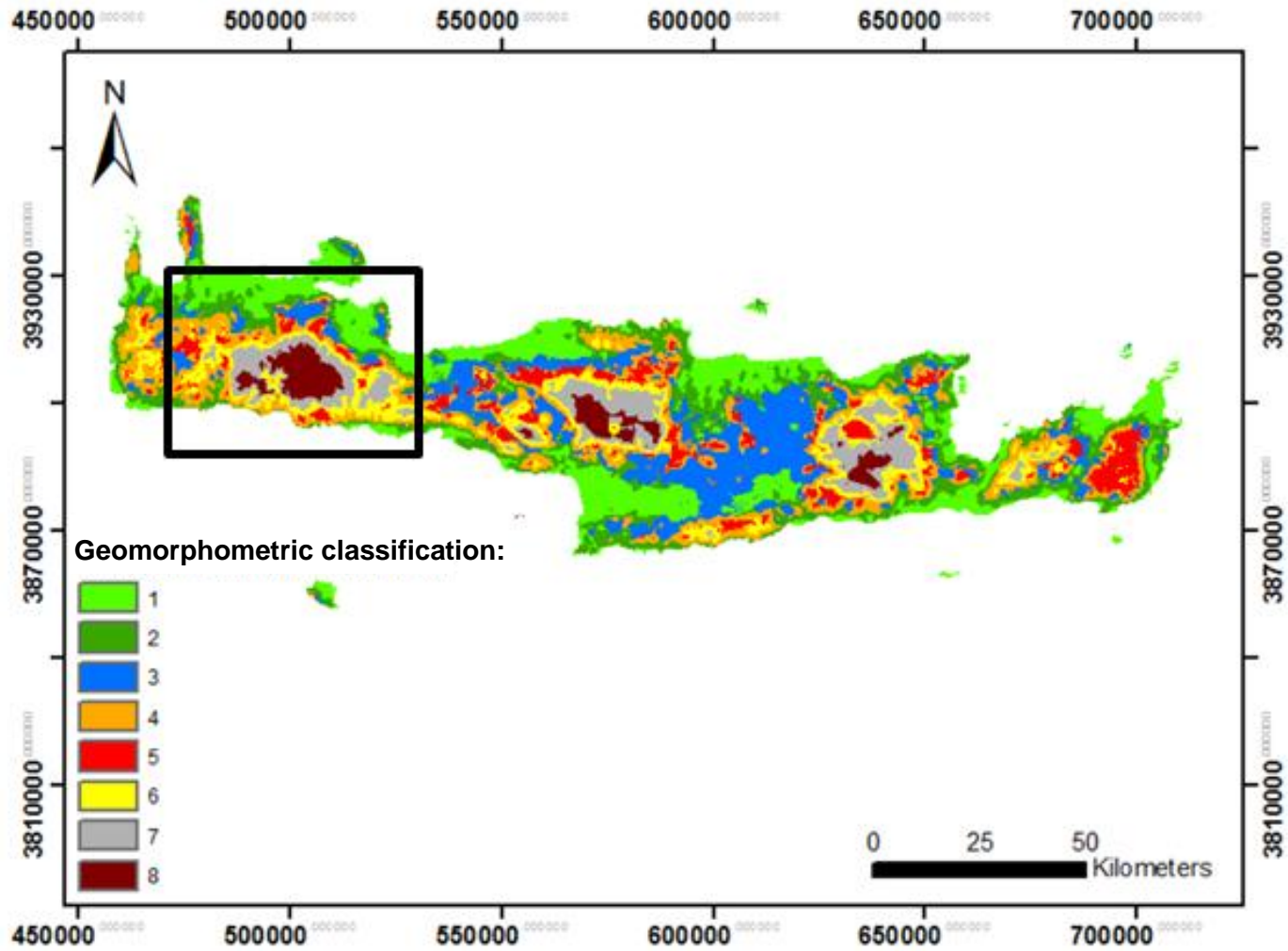
797

798

799

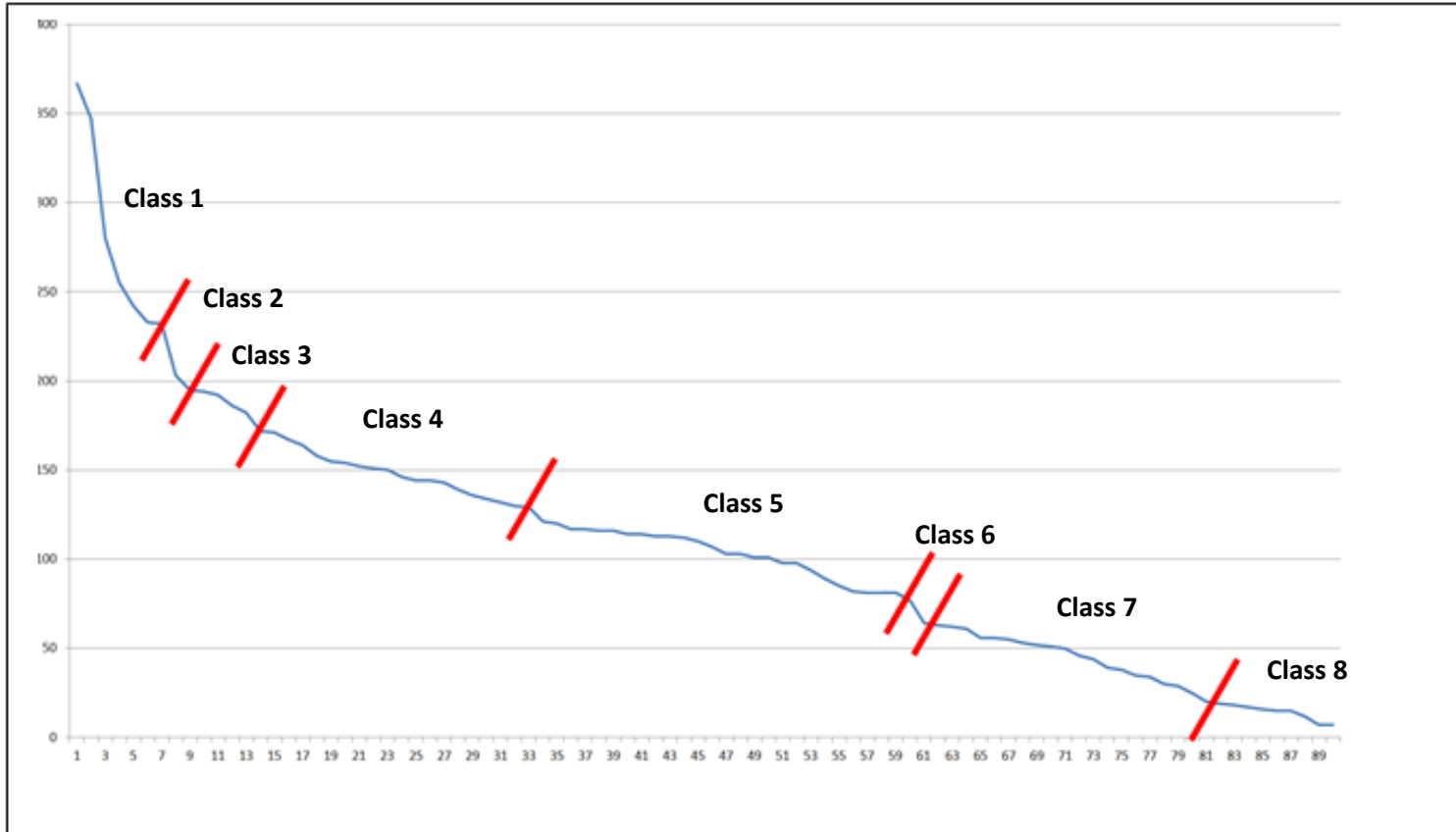
800

(A)



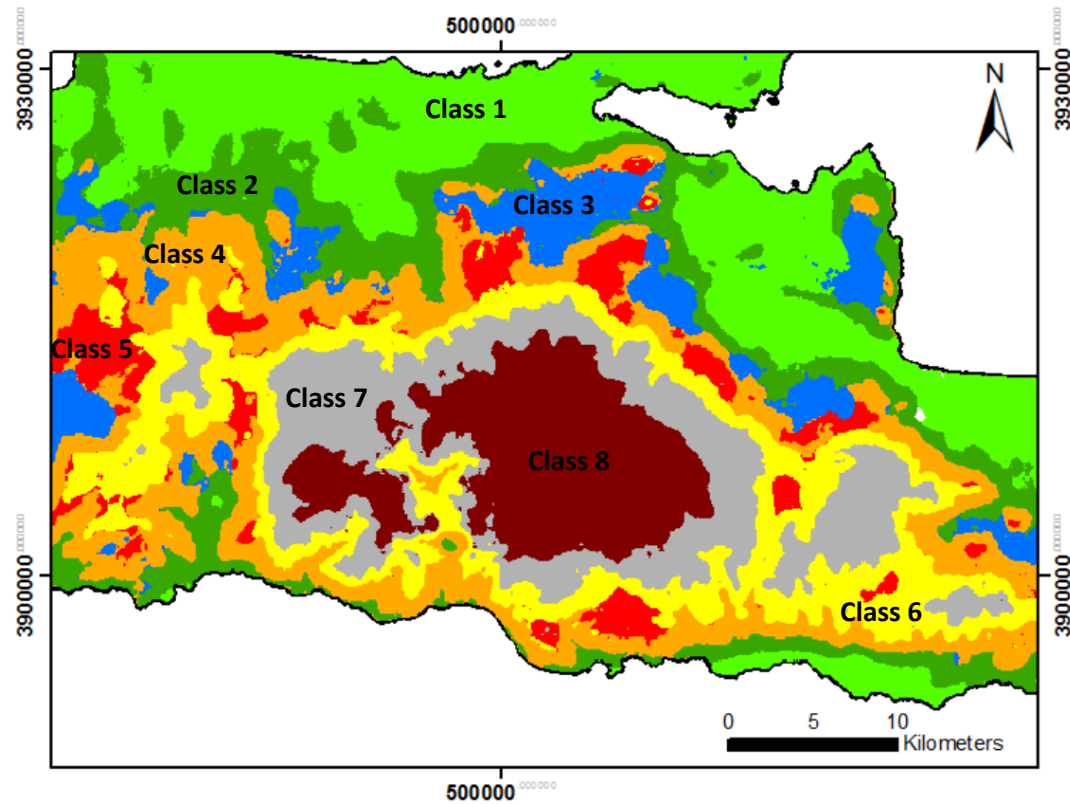
801

(B)



802

(C)

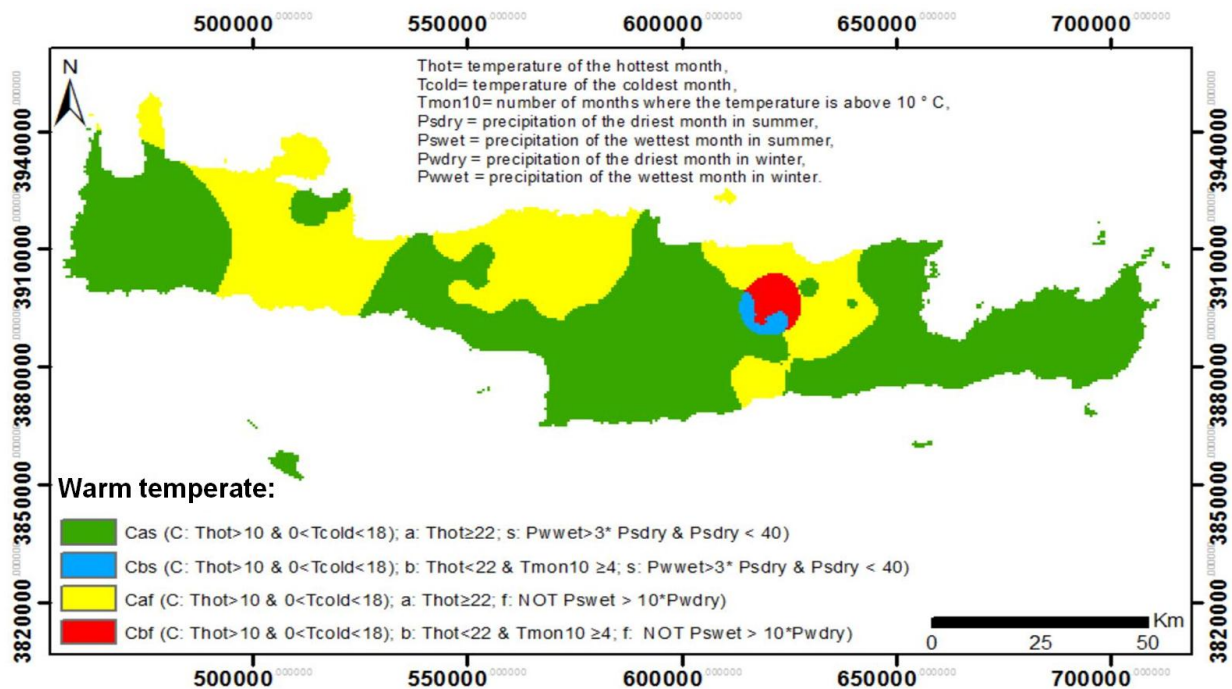


803

804 **Fig. 5 (A):** Regional overview of the results for the ISODATA cluster algorithm for the nine selected geomorphometric indices; **(B):**  
805 the eight derived classes as extracted from the discriminated natural breaks of the clustering histogram curve; **(C):** Zoom-in map  
806 (black square in (A)) of the eight highlighted geomorphometric classes (see Table 2 for legend information).

807

808



809

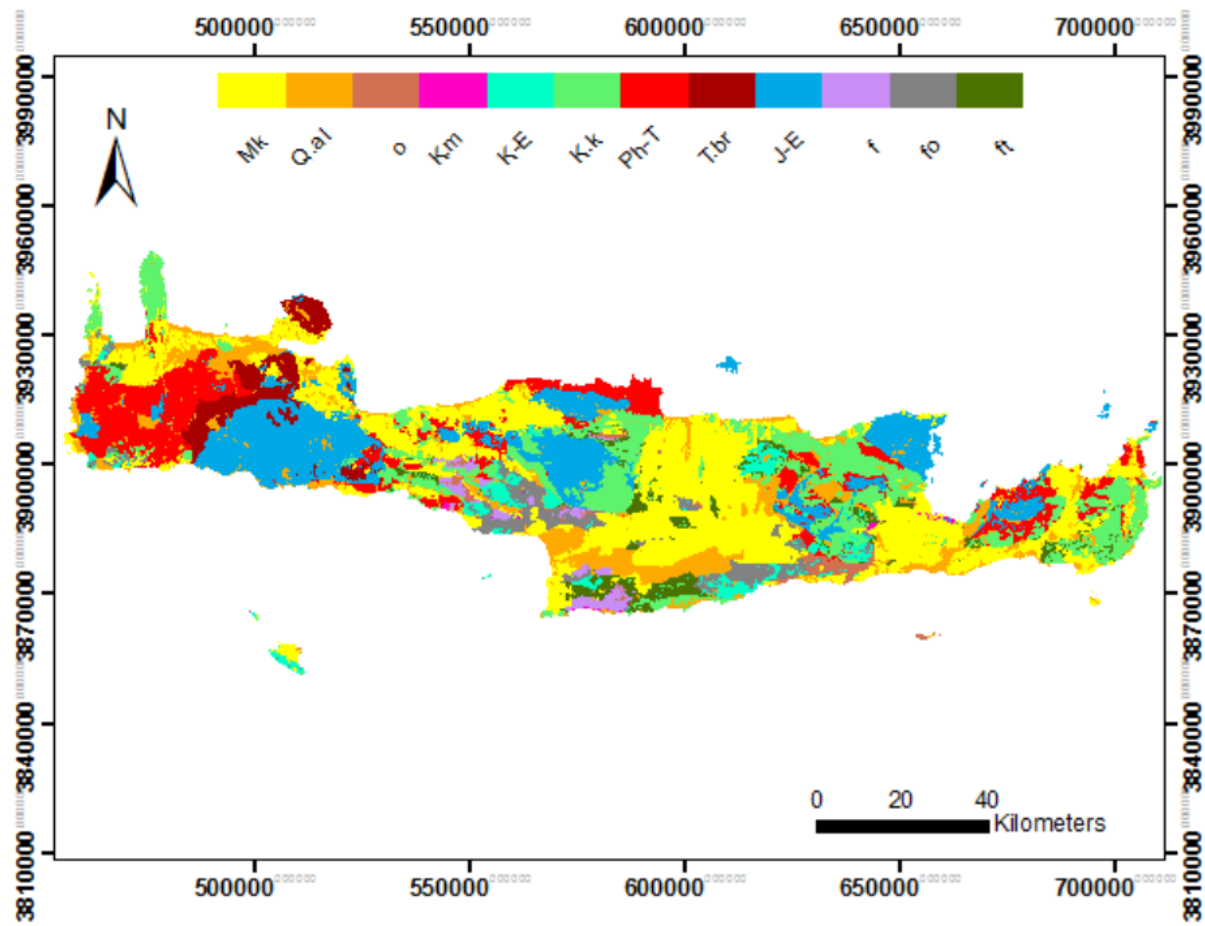
810 **Fig. 6.** Climatic classification, based on precipitation (1930 to 2000) and temperature (1950 to 2000) datasets. The region is  
811 characterized as warm temperate climate, described by *Cas*, *Cbs*, *Caf* and *Cbf* classes.

812

813



814

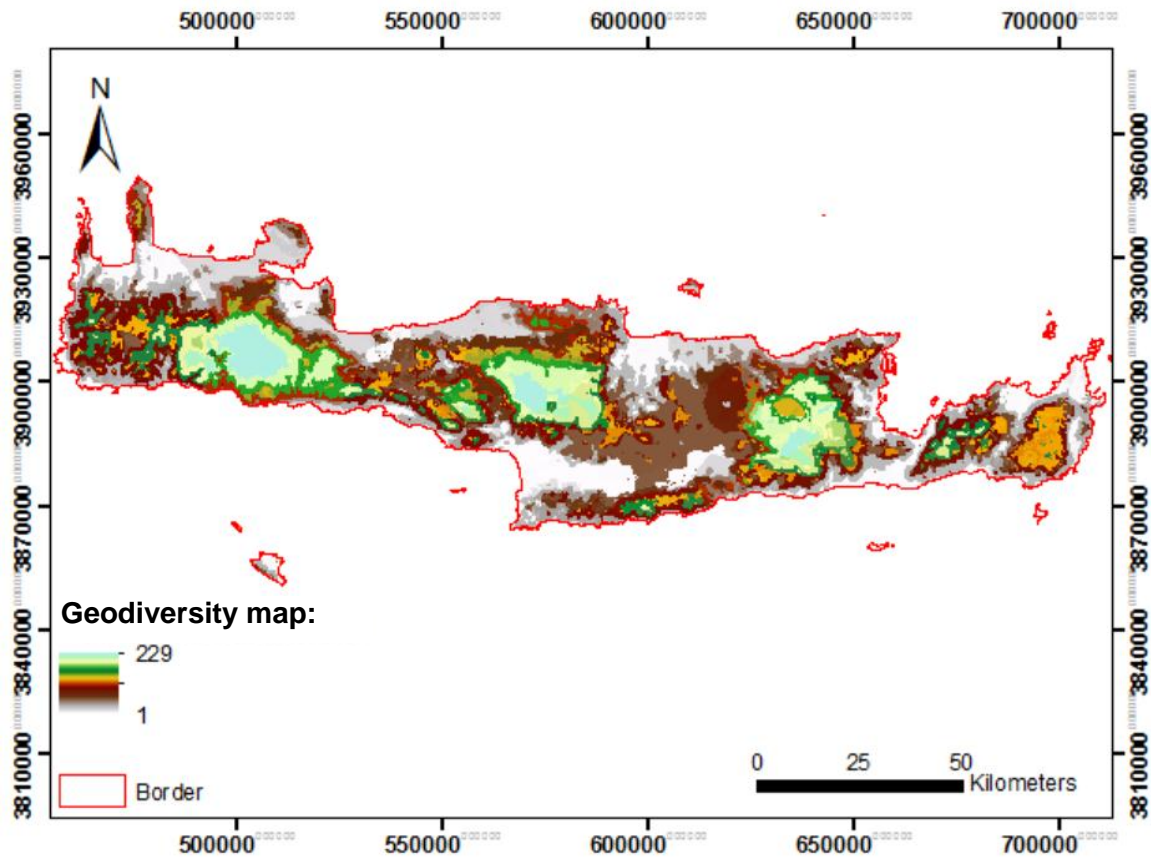


815

816 **Fig.7.** Simplified geological setting based on the classification of the 74 rock formations to 12 main units after Sarris (2007) and

817 Fassoulas et al. (2007) studies.

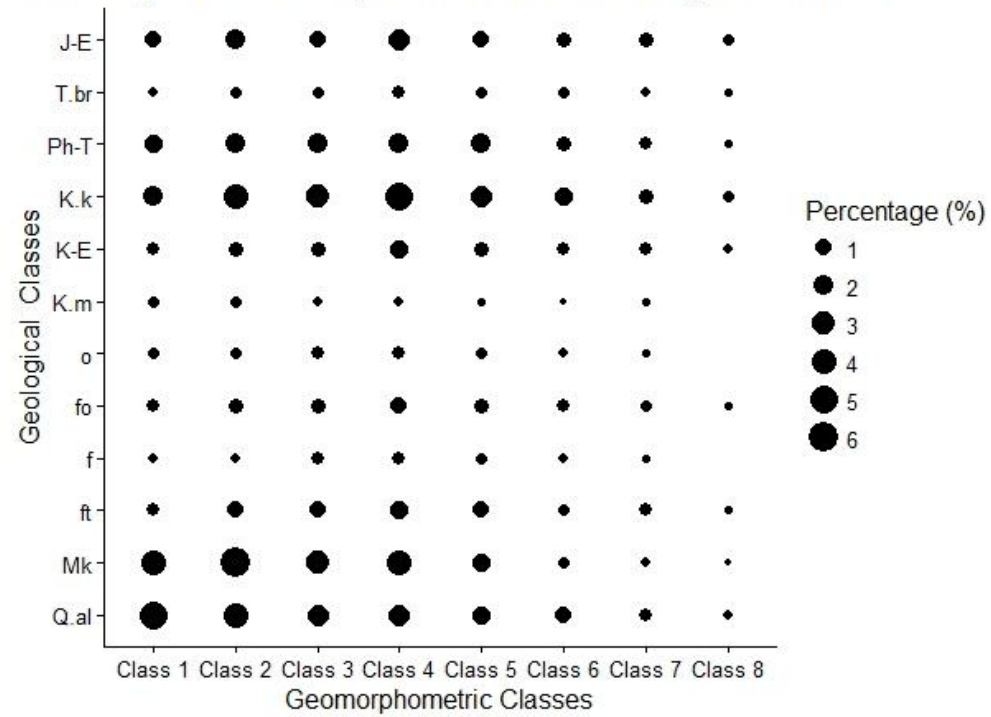
(A)



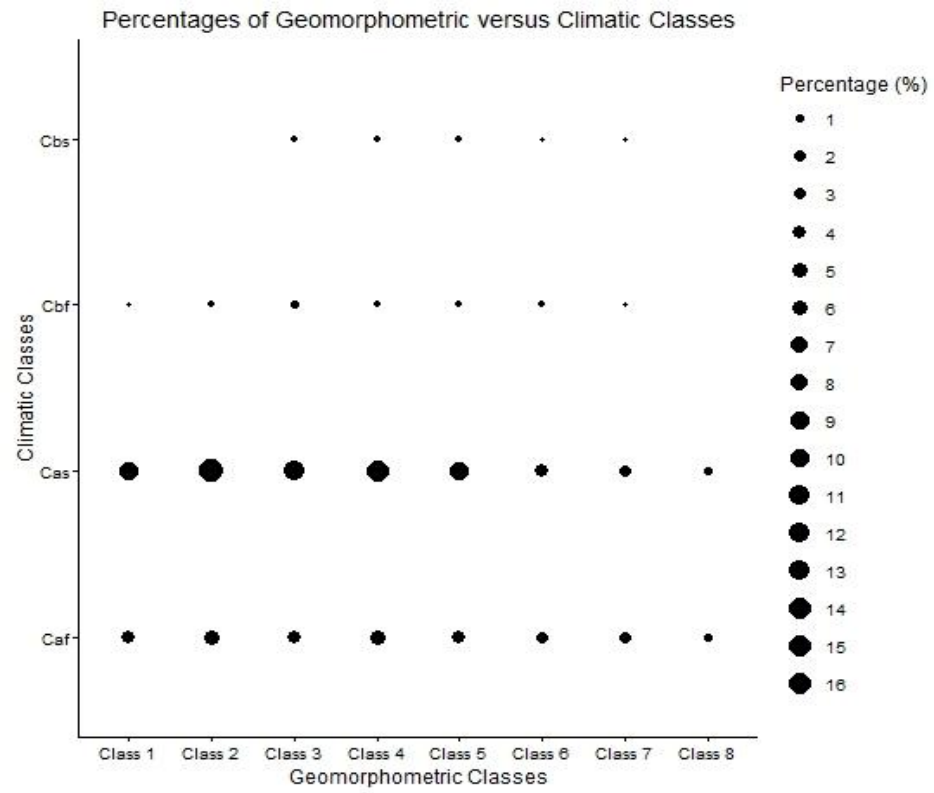
818

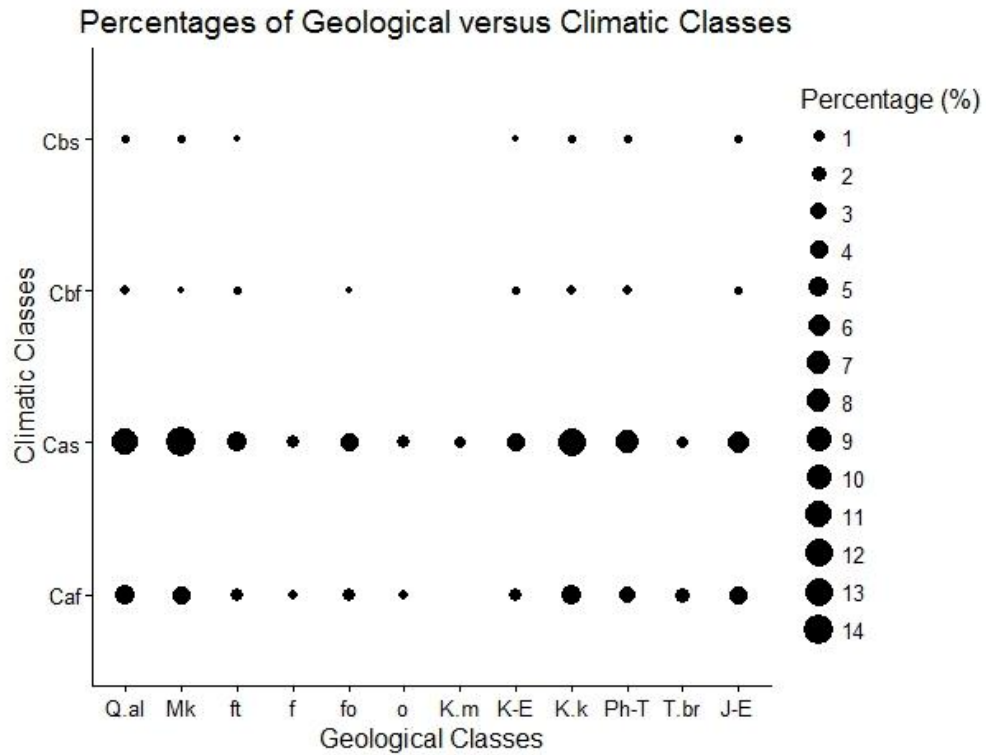
(B)

Percentages of Geomorphometric versus Geological Classes



819





821

822 **Fig. 8. (A)** Geodiversity map, based on the union overlay procedure of the geomorphometric, geological and climatic classifications;

823 **(B)** The occurrences among each of the three classifications acknowledged to the final geodiversity map.

824

825

826

Layer	<i>Ar</i>	<i>SL</i>	<i>Fu</i>	<i>Dd</i>	<i>Er</i>	<i>TWI</i>	<i>Sg</i>	<i>SAR</i>	<i>Di</i>
<i>Ar</i>	1	0.528	-0.056	-0.138	0.022	-0.067	0.585	0.474	-0.048
<i>SL</i>	0.528	1	0.063	-0.045	0.015	-0.033	0.285	0.212	0.365
<i>Fu</i>	-0.056	0.063	1	0.356	-0.002	0.153	-0.061	-0.032	0.215
<i>Dd</i>	-0.138	-0.045	0.356	1	0.004	0.106	-0.157	-0.092	0.14
<i>Er</i>	0.022	0.015	-0.002	0.004	1	-0.217	0.013	0.005	0.016
<i>TWI</i>	-0.067	-0.033	0.153	0.106	-0.217	1	-0.138	-0.093	0.088
<i>Sg</i>	0.585	0.285	-0.061	-0.157	0.013	-0.138	1	0.566	-0.307
<i>SAR</i>	0.474	0.212	-0.032	-0.092	0.005	-0.093	0.566	1	-0.133
<i>Di</i>	-0.048	0.365	0.215	0.14	0.016	0.088	-0.307	-0.133	1

827

828 **Table 1.** Correlation coefficient matrix table highlighting the interdependency of the input dataset layers to be used in the  
829 geomorphometric classification.

830








831


832

833

834

835

<b>Elevation</b>	<b>Class ID</b>	<b>Major geomorphometric units description</b>
Low relief	 1	Coastal lands, alluvial deposits and plains of low height (mean:108m asl), with gentle slopes (mean: 7.8 <sup>0</sup> ), fine drainage texture, low degree of landscape deformation, high moisture accumulation, low degree of dissection or vertical erosion, very low roughness.
Low relief	 2	Plains and valleys with mean height 208m asl, moderate slopes (mean: 17 <sup>0</sup> ), very low degree of dissection or vertical erosion, permeable surface material, high infiltration capacity, moderate roughness.
Low relief	 3	Hillsides and slope valleys with mean height 371m asl, gentle slopes (mean: 10 <sup>0</sup> ), moderate degree of dissection or vertical erosion, low roughness.
Intermediate relief	 4	Hillsides and slope valleys with mid heights (mean: 493m asl), steep slopes (mean: 21 <sup>0</sup> ), coarse drainage texture, high degree of landscape deformation, low degree of dissection or vertical erosion, high roughness.
Intermediate relief	 5	Intermediate plateaus and plains (mean: 617m asl), gentle slopes (mean: 11 <sup>0</sup> ), high moisture accumulation, low degree of landscape deformation, high degree of dissection or vertical erosion, impermeable surface material, low infiltration capacity, low roughness.
Intermediate relief	 6	Hillsides and slope valleys with mid to high heights (mean: 838m asl), steep slopes (mean: 22 <sup>0</sup> ), presence of V-shaped valleys characterized by high incision, low moisture accumulation and longitudinal ridges, moderate degree of dissection or vertical erosion, high roughness.
High relief	 7	Regions with mean height 1188m asl, steep slopes (mean: 20 <sup>0</sup> ), high degree of landscape deformation, presence of V-shaped incised valleys, low moisture accumulation and longitudinal ridges, high degree of dissection or vertical erosion, high roughness.

High relief	 8	Regions with maximum heights (mean: 1745m asl), steep slopes (mean: 24 <sup>0</sup> ), high degree of landscape deformation, presence of V-shaped incised valleys, low moisture accumulation and longitudinal ridges, very high degree of dissection or vertical erosion, maximum roughness.
-------------	---	--

838 **Table 2.** Final geomorphometric classification and description of the eight major geomorphometric classes obtained after the  
839 application of the ISODATA algorithm.

840

1 <sup>st</sup>	2 <sup>nd</sup>	3 <sup>rd</sup>	Description	Criteria*
C			Warm temperate climate	
	a		Hot Summer	$T_{hot} \geq 22^0$
	b		Warm Summer	Not (a) & $T_{mon10} \geq 4^0$
		s	Dry Summer	$P_{sdry} < 40mm$ & $P_{sdry} < P_{wwet}/3$
		w	Dry Winter	$P_{wdry} < P_{swet}/10$
		f	Without dry season	Not (Cs) or (Cw)

841

842 **Table 3.** Updated Koppen-Geiger classification based on climate types and defining criteria (after Kottek et al., 2006). \*:  $T_{hot}$ =  
843 temperature of the hottest month;  $P_{sdry}$ = precipitation of the driest month in summer;  $P_{wdry}$ = precipitation of the driest month in winter;  
844  $P_{swet}$ = precipitation of the wettest month in summer;  $P_{wwet}$ = precipitation of the wettest month in winter;  $T_{mon10}$ = number of months  
845 where the temperature is above 10<sup>0</sup>.

846



Age	Geological units	Geomorphometric classes percentage (%) for each geological unit								Total area coverage (%) of each geological unit
		Class 1	Class 2	Class 3	Class 4	Class 5	Class 6	Class 7	Class 8	
Cenozoic	Quaternary ( <i>Q.al</i> )	55.6	12.13	15.48	6.44	5.51	2.34	2.4	0.06	11.01
Cenozoic	Neogene ( <i>Mk</i> )	38.07	20.84	26.77	6.88	4.82	1.51	1.09	0.0005	29.08
Cenozoic	Flysch Tripolis zone ( <i>ft</i> )	3.64	22.15	24.91	20.59	11.51	11.23	5.2	0.76	3.31
Mesozoic	Flysch-Schist allochthonous series ( <i>f</i> )	10.92	26.53	19.27	28.36	9.72	5.02	0.15	-	1.42
Mesozoic	Flysch Pindos zone ( <i>fo</i> )	6.85	25.92	17.97	32.24	8.84	6.33	1.57	0.24	3.81
Mesozoic	Ophiolites allochthonous series ( <i>o</i> )	7.73	18.48	14.76	34.37	20.68	3.37	0.57	-	1.13
Mesozoic	Carbonate allochthonous series ( <i>K.m</i> )	28.53	42.5	3.71	2.23	1.2	1.01	20.81	-	0.16
Mesozoic	Carbonate Pindos zone ( <i>K-E</i> )	2.82	13.92	19.36	21.52	4.81	19.9	13.34	4.3	3.01
Mesozoic	Carbonate Tripolis zone ( <i>K.k</i> )	7.48	16.04	10.42	21.6	11.64	12.16	14.9	5.73	15.1
Mesozoic	Phyllite-Quartzite series ( <i>Ph-T</i> )	7.84	23.39	11.28	32.29	8.39	14.13	2.6	0.04	12.15
Mesozoic	Carbonate Tripali zone ( <i>T- Br</i> )	11.32	13.4	12.01	14.96	6.75	17.48	20.21	3.84	3.61
Palaeozoic	Plattenkalk nappe ( <i>J-E</i> )	3.8	10.24	6.4	17.37	5.99	17.52	21.34	17.31	16.21

847

848 **Table 4.** The geomorphometric classes areal distribution over each of the twelve geological units and the total area coverage (%) of  
849 each geological unit across Crete.

850

851

852

853

Landscape metric	Range	Description
<b>Patch Richness Density (PRD)</b>	$PRD > 0$ , without limit	$PRD$ equals the number of different patch classes present within the landscape boundary, divided by total landscape area ( $m^2$ ), multiplied by 10000 and 100 (to convert to 100 hectares). It standardizes richness to a per area basis that facilitates comparison of landscapes.
<b>Shannon's Diversity Index (SHDI)</b>	$SHDI \geq 0$ , without limit $SHDI = 0$ , when the landscape contains only one patch (no diversity)	$SHDI$ equals minus the sum, across all patch classes, of the proportional abundance of each patch class multiplied by that proportion. It increases as the number of different patch classes increases and the proportional distribution of area among patch classes becomes more equitable.
<b>Simpson's Diversity Index (SIDI)</b>	$0 \leq SIDI \leq 1$ , $SIDI = 0$ , when the landscape contains only one patch (no diversity)	$SIDI$ equals 1 minus the sum, across all patch classes, of the proportional abundance of each patch class squared. It increases as the number of different patch classes increases and the proportional distribution of area among patch classes becomes more equitable. Represents the probability that any two pixels selected at random would be different patch classes.
<b>Shannon's Evenness Index (SHEI)</b>	$0 \leq SHEI \leq 1$ , $SHDI = 0$ , when the landscape contains only one patch (no diversity), while approaches 0 as the distribution of area among the different patch classes becomes increasingly uneven; $SHDI = 1$ , when distribution of area among patch classes is perfectly even (proportional abundances are the same)	$SHEI$ equals minus the sum, across all patch classes, of the proportional abundance of each patch type multiplied by that proportion, divided by the logarithm of the number of patch classes. It is expressed such that an even distribution of area among patch classes results in maximum evenness. Evenness is the compliment of dominance.
<b>Simpson's Evenness Index (SIEI)</b>	$0 \leq SIEI \leq 1$ , $SIEI = 0$ , when the landscape contains only one patch (no diversity), it approaches 0 as the distribution of area among the different patch classes becomes increasingly uneven; $SIEI = 1$ , when distribution of area among patch classes is perfectly even	$SIEI$ equals 1 minus the sum, across all patch classes, of the proportional abundance of each patch type squared, divided by 1 minus 1, divided by the number of patch classes. It is expressed such that an even distribution of area among patch classes results in maximum evenness. Evenness is the compliment of dominance.
<b>Shape index (SHAPE)</b>	$SHAPE \leq 1$ , without limit. $SHAPE = 1$ when the patch is square and increases without limit as patch shape becomes more irregular.	Equals patch perimeter (m) divided by the square root of patch area ( $m^2$ ), adjusted by a constant to adjust for a square standard.
<b>Proximity index (PROX)</b>	$PROX \geq 0$ , $PROX = 0$ , if a patch has no neighbors of the same patch type within the specified search radius. $PROX$ increases as the neighborhood (defined by the specified search radius) is increasingly occupied by patches of the same type and as those patches become closer and more contiguous (or less fragmented) in distribution. The upper limit of $PROX$ is affected by the search radius and the minimum distance between patches.	Equals the sum of patch area ( $m^2$ ) divided by the nearest edge-to-edge distance squared ( $m^2$ ) between the patch and the focal patch of all patches of the corresponding patch type whose edges are within a specified distance (m) of the focal patch. Note, when the search buffer extends beyond the landscape boundary, only patches contained within the landscape are considered in the computations. In addition, note that the edge-to-edge distances are from cell center to cell center.
<b>Related circumscribing</b>	$0 < CIRCLE < 1$ , $CIRCLE$ approaches 0 for circular patches and approaches 1 for	Equals 1 minus patch area ( $m^2$ ) divided by the area ( $m^2$ ) of the smallest circumscribing circle.

<b>circle (CIRCLE)</b>	elongated linear patches.	854
<b>Perimeter-area fractal dimension (PAFRAC)</b>	$1 \leq PAFRAC \leq 2$ , A fractal dimension greater than 1 for a 2-dimensional landscape mosaic indicates a departure from a Euclidean geometry (i.e., an increase in patch shape complexity). <i>PAFRAC</i> approaches 1 for shapes with very simple perimeters such as squares, and approaches 2 for shapes with highly convoluted, plane-filling perimeters.	Equals 2 divided by the slope of regression line obtained by regressing the logarithm of patch area (m <sup>2</sup> ) against the logarithm of patch perimeter (m). That is, 2 divided by the coefficient b1 derived from a least squares regression fit to the following equation: $\ln(\text{area}) = b_0 + b_1 \ln(\text{perim})$ . Note: <i>PAFRAC</i> excludes any background patches.
<b>Patch density (PD)</b>	<i>PD</i> > 0, constrained by cell size. <i>PD</i> is ultimately constrained by the grain size of the raster image, because the maximum <i>PD</i> is attained when every cell is a separate patch. It expresses number of patches on a per unit area basis that facilitates comparisons among landscapes of varying size.	Equals the number of patches in the landscape divided by total landscape area (m <sup>2</sup> )
		858
		859

860 **Table 5.** Landscape metrics with descriptive details of each index.

861

862

863

864

865

866

867

868

869

870

871

872

(a)		Area (km <sup>2</sup> )	Landscape and patch metrics (Geodiversity map)												
			<i>PRD</i>	<i>SHDI</i>	<i>SIDI</i>	<i>SHEI</i>	<i>SIEI</i>	<i>NP</i>	<i>PD</i>	<i>LSI</i>	<i>SHAPE</i>	<i>CIRCLE</i>	<i>PAFRAC</i>	<i>PROX</i>	<i>COHESION</i>
<b>Crete</b>		8336	0.027	4.32	0.976	0.795	0.98	11682	1.42	62.92	1.52	0.591	1.218	167.9	98.75
<b>District</b>	<b>Chania</b>	2376	0.045	3.78	0.965	0.81	0.974	3144	1.34	33.08	1.53	0.595	1.232	188.4	98.95
	<b>Rethymno</b>	1496	0.099	4.16	0.975	0.835	0.981	2600	1.76	30.74	1.55	0.6	1.212	81.98	98.3
	<b>Herakleio</b>	2641	0.075	3.93	0.951	0.743	0.956	2910	1.10	30.69	1.53	0.591	1.196	245.53	98.96
	<b>Lasithi</b>	1823	0.059	3.72	0.964	0.799	0.973	3231	1.8	34.24	1.49	0.581	1.223	126.35	98.49

873

(b)		Area (km <sup>2</sup> )	Landscape and patch metrics (Geomorphometric classification)												
			<i>PRD</i>	<i>SHDI</i>	<i>SIDI</i>	<i>SHEI</i>	<i>SIEI</i>	<i>NP</i>	<i>PD</i>	<i>LSI</i>	<i>SHAPE</i>	<i>CIRCLE</i>	<i>PAFRAC</i>	<i>PROX</i>	<i>COHESION</i>
<b>Crete</b>		8336	0.01	1.972	0.849	0.948	0.971	17457	2.11	64.25	1.181	0.216	1.459	859.93	98.83
<b>District</b>	<b>Chania</b>	2376	0.003	1.971	0.848	0.948	0.969	4691	1.98	33.53	1.17	0.2136	1.454	903.73	99.01
	<b>Rethymno</b>	1496	0.006	2.007	0.858	0.965	0.981	3062	2.07	26.97	1.19	0.22	1.44	357.44	98.36
	<b>Herakleio</b>	2641	0.003	1.806	0.807	0.868	0.922	6047	2.29	37.07	1.183	0.2198	1.468	1010.2	98.86
	<b>Lasithi</b>	1823	0.004	1.951	0.846	0.938	0.967	3755	2.08	32.18	1.19	0.2195	1.436	401.28	98.54

874

(c)		Area (km <sup>2</sup> )	Landscape and patch metrics (Geological classification)												
			<i>PRD</i>	<i>SHDI</i>	<i>SIDI</i>	<i>SHEI</i>	<i>SIEI</i>	<i>NP</i>	<i>PD</i>	<i>LSI</i>	<i>SHAPE</i>	<i>CIRCLE</i>	<i>PAFRAC</i>	<i>PROX</i>	<i>COHESION</i>
<b>Crete</b>		8336	0.001	2.021	0.834	0.813	0.909	3829	0.459	36.83	1.62	0.61	1.26	1657.97	99.54
<b>District</b>	<b>Chania</b>	2376	0.004	1.811	0.814	0.786	0.905	1141	0.479	19.7	1.63	0.628	1.285	2005.85	99.62
	<b>Rethymno</b>	1496	0.008	1.996	0.833	0.803	0.909	722	0.488	18.93	1.77	0.65	1.287	710.07	99.3
	<b>Herakleio</b>	2641	0.004	1.870	0.779	0.78	0.857	689	0.26	16.27	1.67	0.62	1.253	2056.1	99.65
	<b>Lasithi</b>	1823	0.005	1.725	0.787	0.749	0.875	1407	0.77	21.71	1.5	0.58	1.251	1338.75	99.47

875

876 **Table 6. a)** Landscape and patch metrics for Crete and the individual districts of Crete, based on the geodiversity map of the island; **b)**  
877 landscape and patch metrics for Crete and the individual districts of Crete, based on the geomorphometric classification of the island;  
878 **c)** landscape and patch metrics for Crete and the individual districts of Crete, based on the geological classification of the island.